ROLE OF PAK2 PROMOTING INTRINSIC TUMOR CELL MOTILITY AND WORSENING PATIENT OUTCOMES IN NON-SMALL CELL LUNG CANCER

By

Adam Marc Bissonnette

Thesis

Submitted to the Faculty of the

Graduate School of Vanderbilt University

in partial fulfillment of the requirements

for the degree of

MASTER OF SCIENCE

in

Cancer Biology

May 11, 2018

Nashville, Tennessee

Approved:

David P. Carbone, M.D., Ph.D.

Barbara Fingleton, Ph.D.

Vito Quaranta, M.D.

To my daughter, Harper, whose eyes, smile, and laugh fill my heart,

and

My beautiful wife, Sarah, for remaining patient and supportive throughout this endeavor.

ACKNOWLEDGEMENTS

First and foremost, I would like to thank my advisor Dr. David Carbone for providing me all the necessary resources to carry out my research between Vanderbilt University and Ohio State University. Though I may not have always deserved his support as a graduate student, Dr. Carbone always stood firmly in my corner until the very end even pledging his support for my PhD candidacy after a long period of time with little progress towards the completion of my doctoral requirements. For that, I could not be any more grateful. I am also appreciative of Dr. Barbara Fingleton and Dr. Vito Quaranta, for their work on my dissertation committee, as well as the sharing of their precious time to offer me guidance throughout my graduate studies.

To all of the students, post-docs, and researchers who I have collaborated with and had the good fortune to cross paths with along this journey of mine, all of these experiences allowed me to respect the passage that was graduate school. I am entirely grateful for all the words of advice and encouragement from Dr. Joseph Amann, who was omnipresent in the research lab. His expertise in the laboratory made life for me as a graduate student more enjoyable during periods of experimental trial and error, but above all else, it was his genuine kindness and even-keeled nature presiding over the lab's atmosphere that made going to work an enjoyable and learned experience.

Though not all of my family may have understood what I was doing in my research, and how graduate school life was, they always expressed their support in completing what I started, and I thank each and every one of them for that. To my wife, who has been forever patient in this my longest and toughest journey of my life, I offer endless thanks. Sarah, you have been there for me since day one of graduate school, though neither of us

knew it at first. You have gone from friend to spouse in these nine short years, and your desire to see me happy and successful has always been something I wanted to fulfill completely. My biggest regret is not being able to completely fulfill what we both set out to complete together, graduate school.

TABLE OF CONTENTS

LIST OF TABLES

Table Page

LIST OF FIGURES

Figure Page

CHAPTER 1

INTRODUCTION

Objective

Lung cancer accounts for more cancer-related deaths throughout the United States and the world than any other type of cancer [1, 2]. Despite continued advances in translational research and experimental therapeutics, the 5-year lung cancer survival rate for all comers lags behind other malignancies with similar incidence rates worldwide [2]. The majority of newly diagnosed lung cancer patients present with advanced stage disease, limiting their first-line treatment options to select chemotherapeutic regimens if actionable genetic mutations and brain metastases are absent [3-5]. Even patients who present with early stage lung tumors frequently relapse following cytoreductive surgery, yielding higher mortality rates than equivalently staged breast, colon, or prostate tumors [1]. Sadly, the advances in translational lung cancer research have not yielded the durable clinical responses observed in other oncology clinics.

One of the reasons for poor patient outcomes is the highly metastatic nature of the disease. The ability of lung tumors to metastasize prior to patients presenting with evident clinical symptoms drastically reduces patient survival outcomes. Cancer metastasis, being a complex and poorly understood biological process, involves a series of cell biological processes: invasion, intravasation, lymphatic/blood vessel transportation, extravasation, and colonization [6]. Each of these steps relies on a cell's ability to promote motion, which is regulated in part by signaling kinases including the p21-activated kinases (PAKs).

PAKs are a family of serine/threonine kinases comprised of two groups: Group I includes PAK1, 2, and 3; while Group II includes PAK4, 5/7, and 6 (Figure 1A) [7, 8]. The kinase activity of Group I PAKs is principally regulated by two small Rho GTPases, Rac and Cdc42. External stimuli activate the switch from

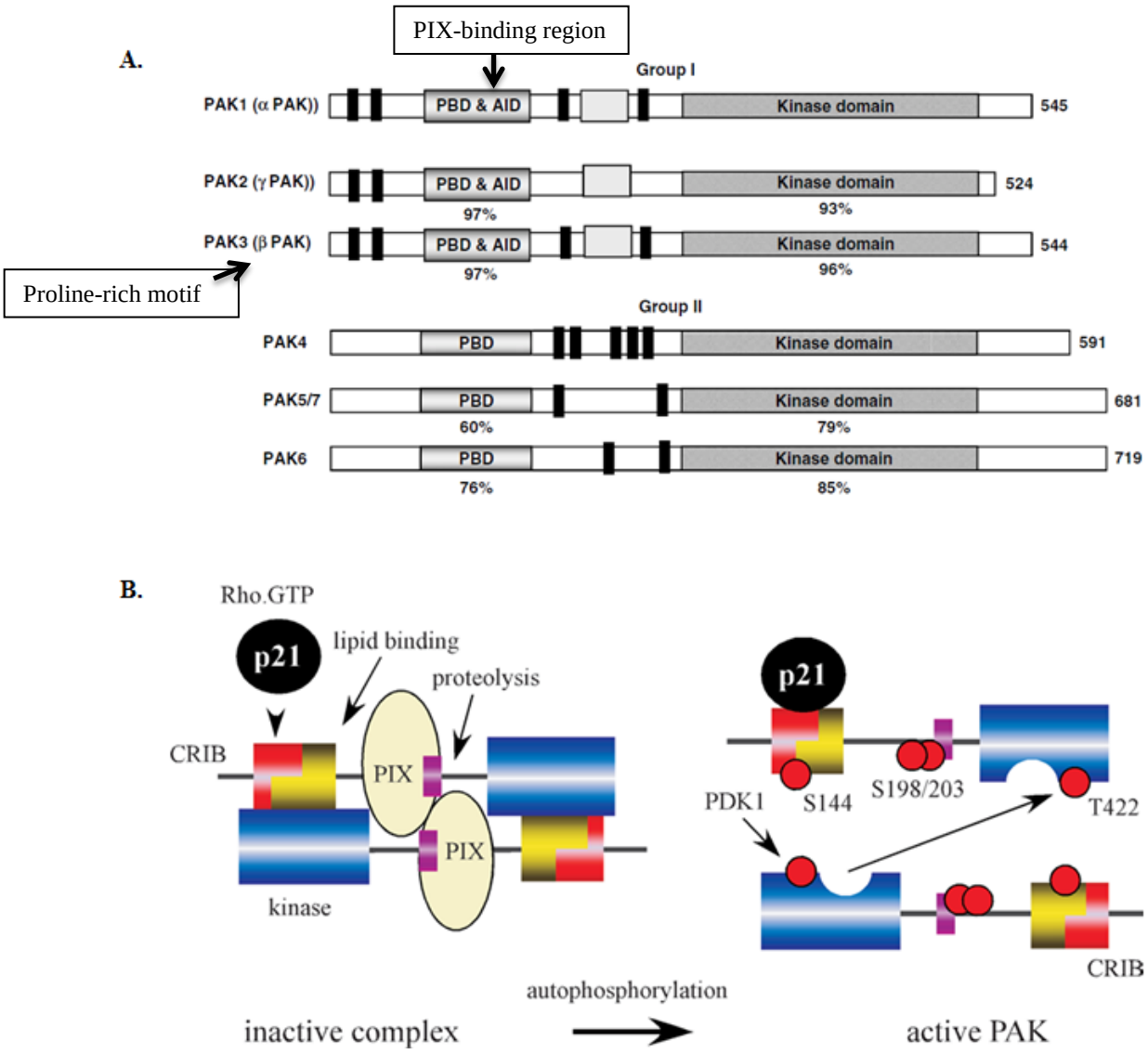

Figure 1. PAK Family Sequence Structure Homology and Kinase Activation Model.

A,Structural domains of group I and group II p21-activated kinases (PAKs). The group I PAKs contain a conserved PBD/AID. Binding of GTPases Cdc42 and Rac to the PBD releases it from the kinase domain. The group II PAKs contain a PBD but lack and AID. Only group I PAKs have PIX-binding region but all PAKs have conserved proline-rich motifs. Percentage similarities within the group for PBDs and kinase domains are indicated. PBD, p21-binding domain; AID, autoinhibitory domain. Figure adapted from Molli, PR et al. [9]

B,A model for PAK1 activation. The auto-inhibited kinase is arranged in head-to-tail fashion, in which the catalytic domain (blue) binds the AID (yellow) and is supported by associated PIX dimers. Upon Cdc42 (or related GTPase) binding, proteolysis, or lipid binding (arrows), the kinase undergoes a conformational change allowing autophosphorylation (red circles). Phosphorylation of Ser-144 serves to disables the AID–kinase interaction, while phosphorylation of Ser-198/203 reduces the affinity for PIX. Figure adapted from Zhao and Manser [8].

GDP to the GTP-bound states of Rac1 or Cdc42, allowing them to bind to the p21-binding domain (PBD) of PAKs. This interaction between PAK and the GTP-bound Rho GTPase triggers a series of phosphorylation events leading to a conformational change in the kinase domain of the p21-activated kinases [10]. Previous reports have shown that phosphorylation of Serine^{144} and Threonine^{423} on PAK1, as well as the homologous residues on PAK2 (Ser^{141} and Thr^{402}), is required for their respective kinase activity (Figure 1B) [11]. Following kinase activation, PAKs phosphorylate downstream effector proteins modulating cellular processes such as actin cytoskeleton rearrangement, proliferation, survival, apoptosis, and cell cycle control [7, 8].

Initial PAK studies centered on their biochemical properties, including activators and inhibitors of catalytic activity, as well as the structural biology of the kinase family. More recently, *PAK* overexpression and hyperactivity has been described in tumor biology [9, 12, 13]. Reports from breast and pancreatic cancer have identified upregulated gene expression in tumor tissue, correlating with progressive disease [14-16]. Additionally, PAK enzymatic activity has been shown to enhance tumorigenicity of known oncogenes, for instance in *KRAS*-dependent transformation of neural Schwann cell tumors and skin squamous cell carcinoma [17-19]. Although PAK biology has been studied in certain cancers, less is known about the role of PAK2 in non-small cell lung cancer (NSCLC). Recent research has described PAK1 and PAK2 overexpression in NSCLC, with studies focusing on PAK1 signaling mechanisms and how it mediated lung tumor growth *in vivo* [20-24]. We set out to investigate the role of PAK2 on NSCLC patient outcomes and its role in lung cancer cell biology. Using two independent clinical lung adenocarcinoma datasets, we identified a negative prognostic effect associated with high *PAK2* RNA expression in patient tumors. We also observed an increase in phosphorylated PAK1 (Ser^{144})/PAK2 (Ser^{141}) expression across a broad panel of NSCLC cell lines along with varying intensities of total PAK1 and PAK2 proteins. To further our investigation, we assessed the impact of PAK2 function on NSCLC cell motility using genetic knockdown and pharmacological inhibition studies. Our findings demonstrate a dependency on PAK2 function for promoting cell motility in a subset of lung cancer cell lines expressing basal levels of phosphorylated PAK1 (Ser^{144})/PAK2 (Ser^{141}).

Evolution of Clinical Biomarkers in Non-Small Cell Lung Cancer

Lung tumor biology continues to see improvements in translational research, but unfortunately patient outcomes linger behind other more easily diagnosed cancers [1]. However, in the past two decades, there have been major breakthroughs in NSCLC therapeutics, specifically with regards to lung adenocarcinoma. The discoveries of novel somatic mutations in epidermal growth factor receptor (EGFR), as well as genetic translocations involving the Anaplastic Lymphoma Kinase (ALK) gene, and the approved use of their respective tyrosine kinase inhibitors (TKIs) have dramatically improved survival outcomes in select patients [25-30]. The development of new and effective drugs is promising, especially when clinicians positively match patients to the treatment plan that has the greatest chance to positively impact their tumor. The identification of predictive biomarkers in clinical diagnostics are the tools oncologists use to guide their treatment plans, substantially reducing a patient's tumor burden and improve their quality of life [31]. As the research and clinical fields continue to evolve in the era of precision medicine, the clinical practice guidelines can change frequently. Between January 2016 and January 2017 alone, there were 5 updates to the National Comprehensive Cancer Network's clinical practice guidelines for NSCLC [32]. The current actionable molecular markers in advanced stage NSCLC are EGFR, ALK, ROS1, Programmed Death Ligand-1 (PD-L1)/Programmed Death - 1 (PD-1). Other actionable mutations in NSCLC are being investigated in ongoing Phase 2/3 clinical trials, but have yet to reach the status of the previously stated genes, including BRAF, RET, and MET [33]. In addition to discovering novel inhibitors for therapy and somatic drug-sensitizing mutations, cancer research investigating patient outcomes associated with genetic signatures can also help guide clinical care decision-making. As the amount of molecular markers grows, the hope is clinical practice guidelines will continue to incorporate these biomarkers with novel and current therapies to improve NSCLC patient care.

EGFR

The Epidermal Growth Factor Receptor (EGFR) is a member of the ErbB family of tyrosine kinase receptors that functions in many aspects of cell biology including, but not limited to, cell proliferation,

adhesion, migration, and survival [34, 35]. When aberrantly overexpressed or mutated, hyperactive EGFR signaling exhibits oncogenic properties. EGFR is overexpressed in approximately 60% of NSCLC samples, and depending on the patient population, mutated anywhere between 10-50% of lung adenocarcinomas [36, 37]. In 2003 and 2004 following early results of phase 2 and 3 clinical trials, two first generation EGFR TKIs, gefitinib and erlotinib, were granted Food and Drug Administration (FDA) approval for use in locally advanced and metastatic NSCLC [25, 38-40]. Tumor objective response rates ranged between 12% and 18% in erlotinib and gefitinib clinical trial cohorts, and with median survival between 7 and 9 months. As results from the clinical trials were being released and shortly after drug approval for use in the metastatic setting, several reports from independent research groups identified the presence of somatic *EGFR* mutations in patient tumors [26, 27, 41]. The exon 19 deletions and exon 18, 20, and 21 insertion/point mutations were activating mutations occurring in patients who responded positively to either of the two EGFR TKIs. Retrospective analyses of tumor samples from the early EGFR TKI clinical trials showed the vast majority of responders had tumors harboring a sensitizing *EGFR* mutation. New trials were later designed to select patients for EGFR TKI therapy based on *EGFR* gene mutation status in order to select out patients who would not derive tangible benefit from therapy.

Although identification of sensitizing mutations to gefitinib and erlotinib increased objective response rates, clinicians also noticed that the responders' survival times were not measurably improved compared to salvage chemotherapy [42]. Investigators following the imatinib treatment paradigm of acquired resistance observed in chronic myelogenous leukemia would re-sequence a patient's tumor following disease recurrence, and a new mutation was discovered in *EGFR*, the T790M point mutation [43, 44]. The T790M mutation altered the binding site of the EGFR TKI preventing the interaction between drug and protein, and thereby hindering the continued response to therapy. New generations of the EGFR TKI came to clinic and exhibited prolonged survival outcomes in patients with both the T790M and EGFR TKI sensitizing mutations. Including erlotinib and gefitinib, there are currently 5 FDA approved EGFR targeted therapies available to select tumor types in NSCLC [45]. One of these third generation EGFR TKI therapies, osimertinib was recently granted FDA approval due to successful objective response rates and prolonged survival in the setting of advanced NSCLC.

In a confirmatory Phase 3 clinical trial, AURA3, osimertinib treated patients experienced a greater than two times longer progression-free survival compared to the cohort receiving standard of care platinum-pemetrexed doublet chemotherapy in EGFR-TKI refractory patients [46]. Unfortunately just as patient tumors developed resistance to erlotinib and gefitinib, the same is already occurring in the third generation EGFR TKI treated cohorts [47]. Continued advances in EGFR TKI biology will hopefully trend towards greater survival times, and improve the patients' quality of life until more breakthroughs can be discovered. The use of molecular markers predicting response to the different EGFR TKIs will greatly assist clinical decisions, and improve the objective response rates to cancer therapies in patients harboring actionable EGFR mutations.

ALK

Anaplastic lymphoma kinase (ALK) is a receptor tyrosine kinase with a single transmembrane domain, and unlike EGFR there is limited information regarding receptor activation and function. In 2007, a Japanese research group identified a fusion gene encoding the entire kinase domain of ALK from a patient with NSCLC [28]. The fusion gene comprised of echinoderm microtubule-associated protein protein-like 4 (EML4) at the amino terminus and the intracellular kinase domain of ALK at the carboxyl-terminus. Since the initial discovery of the EML4-ALK fusion gene, there have been over 20 different n-terminal fusion partners with ALK identified from NSCLC patient tumor samples, but all fusions contained a functional kinase domain of ALK [48]. Though little insight is known regarding the signaling mechanisms of ALK, reports have shown the oncogenic behavior of EML4-ALK fusion gene constructs in mouse model systems and *in vitro* studies [28, 49]. Prior to the development of targeted therapy against ALK kinase activity, a study by Shaw et al. detailed the lack of efficacy with EGFR TKI in EML4-ALK positive patients [29]. Within four years of initial discovery of ALK fusions in NSCLC, the FDA approved of a targeted therapy for ALK+ patients in advanced stage NSCLC. The approval of crizotinib was based on the successful phase 1 and 2 trials where selected patients based on the presence or absence of ALK fusions observed increased objective response rates and prolonged progression-free survival [48]. Crizotinib, unlike erlotinib and gefitinib as first generation EGFR TKIs, is a multiple

tyrosine kinase small molecule inhibitor targeting ALK, ROS1, and MET. More rigorous phase 3 trials in chemotherapy-naive ALK+ patients comparing crizotinib against standard of care platinum-pemetrexed doublet chemotherapy again showed the crizotinib treated arm experienced significantly longer progression-free survival outcomes, approximately 4 months, as well as a greater than 30% increase in the objective response rates [48]. The ability to correctly screen patients for *ALK* fusion rearrangements in the clinic, quickly improved the treatment option for these patients that would have resorted previously to standard of care chemotherapy, and improved the patients' quality of life.

Though crizotinib produced positive results in the clinic, acquired resistance to ALK+ treatment led to tumor recurrence in nearly all patients treated with crizotinib, with the central nervous system being the primary site of metastasis. The three main methods for acquired resistance to crizotinib were new ALK kinase domain and gatekeeper mutations (L1196M and G1269A), *ALK* fusion gene amplification, and lastly alternative pathway activation bypassing the loss of ALK signaling. To this end three second generation ALK TKIs (ceritinib, alectinib, and brigatinib) have received FDA approval for use in patients harboring ALK+ tumors. Each of the three inhibitors exhibit targeted activity against crizotinib-resistant acquired ALK mutations, including L1196M, as well as improved efficacy against ALK+ tumors in the central nervous system [48]. In the ALEX clinical trial comparing alectinib against crizotinib in ALK+ patients in the chemotherapy-naïve setting, only 41% of the patients treated in the alectinib arm have experienced disease progression compared to 68% in the crizotinib cohort. As would be predicted, the alectinib treatment group has exhibited far less central nervous system disease progression (9.4%, 12 month cumulative incidence) compared to the crizotinib cohort (41.4%) [50]. As with the majority of TKIs used in molecularly targeted cancer therapies, the ALK+ patients develop acquired resistance to these second generation therapies, and each inhibitor elicits a different tumor response. Alectinib and ceritinib resistant tumors can develop new ALK mutations or activation of unique secondary signaling pathways [48]. Similar to the treatment history of EGFR mutant NSCLC patients, the story of ALK fusion gene NSCLC therapy is still evolving, but patients are continuing to benefit from the

development of precision medicine treatment plans where clinicians can match patients to the best drug available eliciting a maximal therapeutic response.

ROS1

ROS1 is a receptor tyrosine kinase with sequence homology to ALK and the insulin growth factor receptor families, and recently identified as a novel molecular target in the treatment of NSCLC. In 2007, a ROS1 fusion protein was identified in a NSCLC cell line as well as a primary tumor sample [51]. ROS1 genetic rearrangements occur in approximately 1-2% of NSCLC patients, and they almost exclusively occur in their own unique molecular subset of NSCLC with little to no overlap with NSCLC oncogenic driver mutations [52, 53]. ROS1 fusion proteins always contain the entire kinase domain of ROS1, and are situated on the carboxyl terminus. The n-terminal partner gene is most commonly CD74, but there have been 13 other partner genes identified [52]. NSCLC patients diagnosed with a ROS1+ fusion tumor are typically lung adenocarcinomas, and unlike ALK+ tumors occur less frequently outside of the lung, and at significantly lower incidence rates in the brain. Following the discovery of ROS1 fusions in NSCLC, McDermott et al. observed one cell line demonstrated sensitivity to the ALK inhibitor though not possessing an ALK fusion gene [54]. Due to the sequence homology between ALK and ROS1, the investigators hypothesized that the ALK inhibitor induced growth arrest via ROS1 inhibition. Since these pre-clinical findings, NSCLC patients with tumors harboring the ROS1 fusion gene became eligible for enrollment in a Phase I expansion cohort in the Profile 1001 clinical trial to test the efficacy of the multiple TKI crizotinib [55]. Over 70% of the ROS1+ trial participants experienced objective responses to therapy, and 90% of the patients endured stable disease. By 2016, crizotinib was granted FDA approval for patients with ROS1+ tumors, and is currently the only FDA approved therapy for this molecular sub-group of NSCLC. Similar to crizotinib-resistant disease in ALK+ patients, ROS1+ patients also develop TKI resistance. The exact mechanisms are not as well-defined as the EGFR TKI acquired resistance due to the short history of crizotinib-treated ROS1 tumors and the lower prevalence of the disease in the NSCLC population. However, there are two main methods of acquired

Crizotinib resistance in ROS1+ tumors: novel mutations in ROS1 (G2032R, L2026M, and L1951R) and bypass pathway activation [52]. The activation of altered pathways to bypass ROS1 oncogene addiction have only been reported in individual case reports, and have not been as consistently observed in the clinic as have been acquired resistance mutations in *ROS1*. A third method of resistance has been reported where the tumor adopted more mesenchymal features, but has only occurred in one reported instance along with supporting *in vitro* experimental data [52]. As crizotinib continues to make strides in ROS1 rearranged NSCLC patients, new multiple TKI therapies are being tested in early phase 1 and 2 clinical trials aiming to improve cancer care options and outcomes.

PD-L1/PD-1

Programmed death ligand 1 (PD-L1) and its receptor programmed death -1 (PD-1) are immune checkpoint inhibitors expressed on immune cells to control immune reactions during inflammation and prevent against autoimmunity [56]. In tumor biology, PD-L1 is frequently overexpressed on the surface of cancer cells leading to tumor induced immune evasion by binding to the tumor infiltrating lymphocytes. Following ligand-receptor interaction, the receptor internalizes the signal activating the phosphatase SHP2, which dephosphorylates kinases involved in downstream T-cell activation signals [57]. Though the T-cell/tumor cell interaction may have the greatest impact on tumor immune evasion with regards to PD-1/PD-L1 immune monitoring, PD-1 expression on natural killer cells and B-lymphocytes can also further impact a state of immune anergy [56]. The complex, multifactorial behavior of PD-1/PD-L1 immune checkpoint signaling made it an attractive pathway to target in cancer therapeutics. Since the initial clinical trials involving NSCLC opened, four anti-PD-1/PD-L1 therapies have been granted FDA approval in the locally advanced or metastatic NSCLC disease setting: nivolumab, pembrolizumab, atezolizumab, and durvalumab. One of the early hallmarks for these immunotherapies is the duration of the therapeutic response, especially in the heavily pre-treated patient population enrolled in the early phase I clinical trials. For instance, in a dose-escalating phase I trial testing the safety and efficacy of nivolumab, a 17% objective response rate was observed in the patient

population, nearly doubling the average clinical finding in advanced stage chemorefractory NSCLC patients. Even more impressive, patients receiving the dose of drug chosen for further study, 3mg/kg dose of nivolumab, benefitted with an observed 24% objective response rate and 1, 2, and 3 year survival rates of 56%, 42%, and 27% [58]. Each of the immune checkpoint inhibitors granted FDA approval have yielded impressive response rates changing the standard of care for advanced stage NSCLC patients. One of the biggest challenges though in the field of NSCLC immunotherapy is determining how to match this new class of immune checkpoint inhibitors to the correct patient.

Unlike the identification of EGFR TKI sensitizing mutations, there has not been a true predictive biomarker for an anti-PD-1/PD-L1 therapeutic response [45, 59]. Though there does appear to be a positive association between tumor or tumor infiltrating lymphocyte PD-L1 expression and response to targeted PD-1/PD-L1 therapies, patients with negative PD-L1 expressing tumors have also experienced durable responses to this class of immune checkpoint inhibitors [45]. Possible explanations are temporal and spatial changes involved with PD-L1 expression within the tumor and the tumor microenvironment between the tissue biopsy used for diagnostic staining and the expression levels of these co-inhibitory ligands at time of treatment. Unlike say expression of the clonal populations of EGFR mutant lung adenocarcinomas, the expression levels of PD-1 and PD-L1 in the tumor and the surrounding tissue are much more dynamic and heterogeneous. More recent pre-clinical research illustrates the complexity of tumor immunology and the multiple resistance mechanisms that may influence upfront or acquired resistance to immunotherapy. The presence of regulatory T-cells in a tumor can negatively affect the ability to initiate an anti-tumor immune effect, as well as the cytokine milieu secreted by the tumor infiltrating lymphocytes and the tumor itself [60]. In addition to improving the universality of measuring PD-L1 expression within the tumor and the tumor infiltrate, a new predictor of response to immune checkpoint inhibition is the assessment of the tumor mutation burden. In the Checkmate 026 trial, the investigators observed a nearly 4 month increase in median progression-free survival with nivolumab intervention compared to standard of care chemotherapy within the subset of patients afflicted with a high level of non-synonymous tumor mutations [61]. A second study showed strong concordance between

durable response to immune checkpoint inhibitors and the presence of a high tumor mutation burden [62]. To control if the tumor mutation burden was prognostic rather than predictive, they determined that patients with a high tumor mutation burden who did not receive anti-PD-1/PD-L1 therapy experienced worse survival outcomes illustrating that tumor mutation burden did not affect survival regardless of therapeutic intervention. The predictive quality of tumor mutation burden compared equally to the predictive power of tumor PD-L1 expression towards response to PD-1/PD-L1 signaling blockade. To this end, future studies may combine tumor PD-L1 expression score with tumor mutation burden, to enhance patient selection for immunotherapy.

BRAF

BRAF is a serine/threonine kinase involved in the RAS/RAF/MEK/ERK signal transduction pathway that is commonly activated by oncogenic activating mutations. Though *BRAF* mutation more commonly occurs in melanoma, genomic profiling has illustrated up to 3% of NSCLC tumors contain $BRAF^{V600E}$ mutations [63]. Similar to other driver oncogenes, the mutations are generally mutually exclusive to other known genetic drivers of disease (EGFR, ALK, and ROS1). Using a combinatorial approach to targeting $BRAF^{V600E}$ positive tumors and the RAS/RAF/MEK/ERK pathway, a recent clinical trial showed successful survival outcomes with dual inhibition of BRAF and MEK in previously untreated advanced stage NSCLC patients [64]. 64% of patients receiving dabrafenib plus trametinib observed an objective overall response to treatment that was durable (10.4 months). Though the trial was not randomized to standard of care therapy or placebo, the phase II trial demonstrated similar survival benefits to matched patients treated with inhibitors targeting EGFR, ALK, or ROS1 [64]. Within the past year, the FDA has granted approval for the use of these small molecule kinase inhibitors in combination as a first-line treatment in NSCLC patients with the genomic $BRAF^{V600E}$ mutation [65].

Emergence of p21-Activated Kinase Signaling and Tumor Biology

The small Rho GTPases Cdc42 and Rac1 function as the primary activators of the PAK serine/threonine kinase family [7, 8]. PAK1, 2, and 3 were initially identified by forming complexes with radiolabeled GTP-bound Rac and Cdc42 [66]. PAKs mediate the downstream signaling effects of the GTP-bound small Rho GTPases through their kinase activity. The binding partners and intracellular localization of the PAKs regulate the functional output of the signal transduction pathway. Though there are strong similarities in structure and sequence between PAK1, 2, and 3, there are distinct signaling effects between each of the kinases (Figure 1A). The differences between the Group I PAKs are illustrated by the vastly different effects observed in their respective knockout mouse models [13]. PAK1 knockout mice experience little changes aside from some immune cell defects. The PAK2 knockout mice are embryonically lethal, and PAK3 null mice develop severe mental impairments. PAK2 is unique in its ability to undergo caspase cleavage. PAK2 cleavage produces a constitutively active 34 kDa PAK2 fragment that correlates with induction of cell death. However, active full length PAK2 elicits pro-survival signals [67, 68]. In regards to the principal PAK cellular function, cell migration and motility, PAK1 and PAK2 each signal extensively, and not all in the same manner. In a heregulin stimulated breast cancer setting, PAK1 and PAK2 displayed opposing actions on multiple downstream effectors and cellular functions, including myosin light chain phosphorylation, lamellipodia induction, and RhoA activation [69]. As pleiotropic as PAK signaling is under normal biologic conditions, the depth of PAK signaling and expression grows wider in the cancer setting.

PAKs exhibit strong alterations in levels of expression across various tumor settings. Illustrating the transformative and oncogenic properties of the serine/threonine kinase family is the positive correlation between high PAK expression levels and high grade tumors [12, 15, 70, 71]. Not only do PAKs exhibit increased expression, but the immediate upstream activators of PAKs are also frequently upregulated and correlated with progressive disease [72, 73]. The combination of increased levels of PAK expression and the small Rho GTPases, depict an essential role for heightened functional PAK signaling in tumor biology. Potentially more intriguing is the cooperative behavior between PAK signaling and known driver oncogenes,

KRAS and *EGFR*, and tumorigenic phenotypes, for example the epithelial-to-mesenchymal transition [17-19, 24, 74-76]. Though reports of PAK activity in cancer biology are growing, the development of PAK inhibitors has proved challenging, and future development of PAK inhibitors appears poor [77]. Regardless, analysis of PAKs as prognostic or predictive biomarkers in NSCLC would be beneficial to further understanding the tumor biology.

Proteomic Identification of p21-Activated Kinase 2 Over-Expression in Non-Small Cell Lung Cancer

Our research group previously identified increased PAK2 protein levels in squamous cell lung carcinoma pooled tissue samples from a shotgun proteomic approach looking to discover novel candidate biomarkers differentiating between lung adenocarcinoma and squamous cell lung carcinoma, as well as normal lung [20]. The proteomic approach employed showed robustness for identifying peptides previously known to be overexpressed in lung tumors (Aldo-Keto Reductase Family 1, member B10; and Proliferating Cell Nuclear Antigen) as well as novel candidate biomarkers to distinguish between the two major sub-types of NSCLC and non-involved lung tissue. Initial preliminary analysis also identified an increase in PAK1 peptides, but after a more refined statistical cut-off threshold was used, PAK1 fell out from the final analysis. With the finding of PAK2, it drew our interest due to reports from breast and pancreatic cancers showing an active role for PAKs in disease progression and greater cancer cell migration and invasion [14-16]. *In vitro* cell line analysis of PAK2 knockdown and pan-PAK inhibition demonstrated deleterious cell motility effects. However, no correlation was observed between PAK2 tissue immunohistochemistry expression levels and clinical correlates.

Rationale for Current Studies

With the findings from Kikuchi et al. we sought to further investigate the role serine/threonine kinases PAK2 and PAK1 may play as active signaling proteins involved in cell migration and motility in NSCLC. Though PAKs function in various cellular pathways aside from cell motility, their most well-studied kinase targets and effectors involve actin cytoskeleton rearrangement and cell motility to the greatest degree. Our

initial studies sought to measure not only total protein levels for PAK1 and PAK2, but also the basal levels of activated phosphorylated PAK1(Ser^{144})/PAK2(Ser^{141}) in a panel of NSCLC cell lines prior to starting functional assays. The phosphor-serine$^{144/141}$ was selected due to the reports of its requirement for PAK1/2 kinase activity, as it blocks the kinase inhibitory domains from binding to the kinase domain of a neighboring PAK1 or PAK2 protein (Figure 1B) [8, 11]. Our research displayed in this report aims to explore the value of PAK1 and PAK2 kinase function in a cell migration manner in the disease setting of NSCLC, and how to improve its standing as a candidate biomarker in lung adenocarcinoma and squamous cell carcinoma.

CHAPTER 2

INTRINSIC CELL MOTILITY AND PAK2 FUNCTION IN NON-SMALL CELL LUNG CANCER

Introduction

Cancer cell metastasis is the fundamental poor prognostic indicator for cancer survival. Of the fifteen different cancer types assessed by Siegel et al., only four have 5-year survival percentages reaching 30% or better when there is metastatic disease at initial diagnosis [1]. As tumors spread, the ability to curatively treat patients declines considerably. In lung cancer, even though there are a growing number of therapies for advanced stage disease due to the advent of precision medicine and targeted therapies, the rate of recurrence is nearly 100% and eventual patient death is measured in months unfortunately. The goal of our research group is to identify novel biomarkers of lung cancer, and better understand their biological function in promoting tumor development. To that end, our group identified PAK2 to be overexpressed both in lung adenocarcinoma and squamous cell carcinoma using a proteomic mass spectroscopy platform [20]. We hypothesized that PAK2 overexpression in lung cancer would promote increased cell motility and adversely affect patient outcomes in NSCLC. To this end, we evaluated *PAK2* mRNA expression in two independent lung adenocarcinoma datasets as well as a large cohort of lung squamous cell carcinoma patients, each with clinical covariates and survival outcomes. We also determined with *in vitro* cell line studies that basal levels of phosphorylated PAK1 (Ser^{144})/PAK2 (Ser^{141}) defines a subset of lung cancer cells showing greater dependence on PAK2 function for promoting cell motility.

Materials and Methods

In Silico Dataset Analyses

Early stage lung tumors (n=443) with gene expression and clinical covariates were accessed from the

Director's Challenge Consortium for the Molecular Classification of Lung Adenocarcinoma (https://caintegrator.nci.nih.gov/caintegrator/). Microarray expression values were $\log_2$ transformed prior to further analyses. Patients were divided into three equal groups of high, intermediate, or low *PAK2* expression. Since low and intermediate patients did not separate, they were grouped together for univariate Kaplan-Meier survival analysis. A parallel analysis was performed for *PAK1* expression.

Using cBioPortal for Cancer Genomics (www.cbioportal.org), Kaplan-Meier plots for patient overall survival were generated. Patient cohorts were selected from the Lung Adenocarcinoma (TCGA, Nature 2014) and Lung Squamous Cell Carcinoma (provisional) [78-80]. Elevated gene expression samples were defined as having a Z-score ≥ 2.0 in RNAseq expression analysis, or having chromosomal gains as measured by copy number analysis. Additionally, reverse-phase protein array (RPPA) data from the same dataset was mined for further analysis. All data used in this report was accessed from cBioPortal on January 30, 2018.

Cell Culture

HARA and RWGT2 cell lines were generously shared by Dr. Gwendolyn Lorch (Ohio State University, Columbus, OH). The H1703 and H2172 cell lines were provided by Dr. S. Patrick Nana-Sinkam (Ohio State University, Columbus, OH). All additional cell lines were supplied by Drs. John Minna and Adi Gazdar (University of Texas, Southwestern, Dallas, TX). Cell lines were tested for mycoplasma, and confirmed negative for infection (Lonza Walkersville, Inc.). All cells were cultured with media according to recommended suggestions, and maintained at 37˚C in a humidified 5% CO_2 environment.

Two separate pan-PAK inhibitors were used to assess PAK function *in vitro*. PF-3758309 is an ATP-mimetic PAK inhibitor provided from Genentech (South San Francisco, CA). IPA-3 (1,1'-Disulfanediyldinaphthalen-2-ol) is an allosteric inhibitor of the Group I PAKs (Sigma Aldrich, St. Louis, MO). Both drugs were reconstituted in sterile-filtered dimethyl sulfoxide (DMSO).

Immunoblots

Cells were harvested in 6 or 10-cm dishes following two washes with cold 1XPBS, and lysed with a mild cell extraction buffer (0.5% Triton X-100, 0.1% SDS, 0.1% Deoxycholic Acid in PBS supplemented with protease and phosphatase inhibitors). Lysates were sonicated by 10 repeated 1 second bursts, and cleared by centrifugation at 13,000 rpm for 15 minutes at 4˚C. Protein concentrations were measured by DC Protein Assay (Bio-RAD, Hercules, CA). Equivalent amounts of protein were loaded in pre-cast sodium dodecyl sulfate-polyacrylamide gel electrophoresis (SDS-PAGE) gels (Bio-RAD, Hercules, CA). Following blocking, membranes were probed using the following antibodies: PAK1, PAK2, phospho-PAK1 (Ser^{144})/PAK2 (Ser^{141}) (Cell Signaling Technology, Danvers, MA); GAPDH (Santa Cruz Biotechnology, Santa Cruz, CA); β-Actin (Sigma-Aldrich, St. Louis, MO). HRP-conjugated mouse or rabbit secondary antibodies were purchased from GE Healthcare (Buckinghamshire, UK).

Transfections and Stable Cell Knockdowns

PAK1, PAK2, and non-target Mission shRNA expression constructs were purchased as glycerol stocks from Sigma-Aldrich (St. Louis, MO). shRNA and packaging vectors (pMD2.G and pCMV dR7.74ps PAX2) were co-transfected into 293FT cells by calcium phosphate methodology. Culture medium was changed 6 hours following transfection, and lentiviral media collected from transfected cells 48 hours post-transfection. Lentiviral media was centrifuged for 5 minutes at 1600 rpm, and passed through a 45 μm syringe-filter. Polybrene [8μg/mL] was added to the lentiviral media prior to NSCLC cell line infection. Viral media infected target cells when 50-70% confluent for 4-6 hours, and then replaced with standard cell culture media for 48 hours prior to puromycin selection.

Transwell Boyden Chamber Migration Assay

For the migration assay, $5x10^4$ or $1x10^5$ cells were seeded on 8 μm pore membrane transwell inserts in 24-well plates, and then serum-starved for 18-24 hours (Costar, Corning, NY). To stimulate cell migration, a 1-

10% serum gradient was applied between the top and bottom levels of the porous membrane. Cells were assessed for migratory capacity following 18 hours. Cells not passing through the membrane were removed by cotton swab. Filters were placed in 100% methanol for fixation, and then through a series of washes with milliQ water before staining cell nuclei with hematoxylin. Transwell filters were cut from inserts, and mounted onto microscope slides with Aqua-Poly/Mount (Polysciences, Warrington, PA). Twenty random fields were selected to count cells by light microscopy using a 40X oil immersion objective lens (Nikon Eclipse E600).

Wound-Healing Assay

H1703 and H2882 cells were seeded in 24 well plates, and allowed to grow until reaching 100% confluency. Using a P200 pipet tip, a scratch was made thru each well, and washed twice with 500 µl 1XPBS and once with 500 µl RPMI to remove floating cells. Control and experimental media were added to cells, and images taken at two time points to assess wound closure at 4X magnification (Nikon Eclipse TE2000-U). Four fields were assessed per treatment group. A QImaging Micropublisher 3.3 camera along with QCapture Imaging software was used for acquiring representative images in each well (QImaging, Surrey, British Columbia, Canada). ImageJ software was used to calculate wound area by analyzing initial and final time point images.

Aligned Nanofiber Three-Dimensional Cell Motility Assay

Adhered lung cancer cells on aligned nanofiber substrates were visualized for tracking cell migration using time-lapse confocal microscopy using methods previously described [81, 82]. Confocal microscope (Olympus IX73) images using a 10X objective and fluorescence excitation/emission wavelengths of 480/520 nm were taken from three distinct regions of interest per well every 30 minutes over a 24 hour period. Sequential images were stitched together to form a video for cell migration tracking analysis with utilization of the MTrackJ software plugin for ImageJ. 25 cells per video were selected and their displacement vectors were tracked and recorded with respect to time. The average total migration distance in microns and average velocity

in microns per hour were reported with standard deviations for each of the NSCLC cell lines assayed.

Statistical Analyses

All statistical analyses were performed using either Minitab16 (State College, PA), SPSS (Chicago, IL), or GraphPad Prism 5 version 5.02 for Windows (San Diego, CA). Unpaired student's t-tests were performed to compare statistical differences between non-target and knockdown cells in transwell and wound-healing cell migration assays. For 3D live cell tracking, an analysis of variance (ANOVA) was utilized to compare the differences in the means of the variables. In addition, a single and cooperation variable analysis was conducted using the Tukey's test to determine unique statistical significance between untreated and treated cell line samples. All results were presented as mean value and the standard deviation. Kaplan-Meier survival, Fisher's exact test, and Cox regression analyses were performed using SPSS software (Chicago, IL). Log-rank test statistics were applied to measure differences between patient groups on Kaplan-Meier plots. All ρ-values < 0.05 indicated a significant difference between study groups.

Results

Negative Clinical Impact Associated with Elevated *PAK2* Gene Expression in Lung Adenocarcinoma

Using publically available patient follow-up and microarray data from the Director's Challenge Consortium, we performed Kaplan-Meier survival analysis stratifying patients by *PAK1* or *PAK2* RNA expression levels (Fig. 2A). In our initial univariate analysis, *PAK2* expression significantly associated with a worse clinical outcome as evidenced by a greater than 30 month reduction in median overall survival (mOS) in patients with high *PAK2* levels (Table 1, 45.8 vs. 79.5 months, Log-rank $\rho = 0.001$). A multivariate Cox regression analysis revealed *PAK2* expression affected survival independent of age, gender, and stage (Table 2, HR = 1.54, 95% CI, 1.150 – 2.062, $\rho = 0.004$). Stratifying patients by *PAK1* RNA levels showed no difference between the two patient groups (Table 1, Fig. 1A, 65.0 vs 71.0 months, Log-rank $\rho = 0.547$).

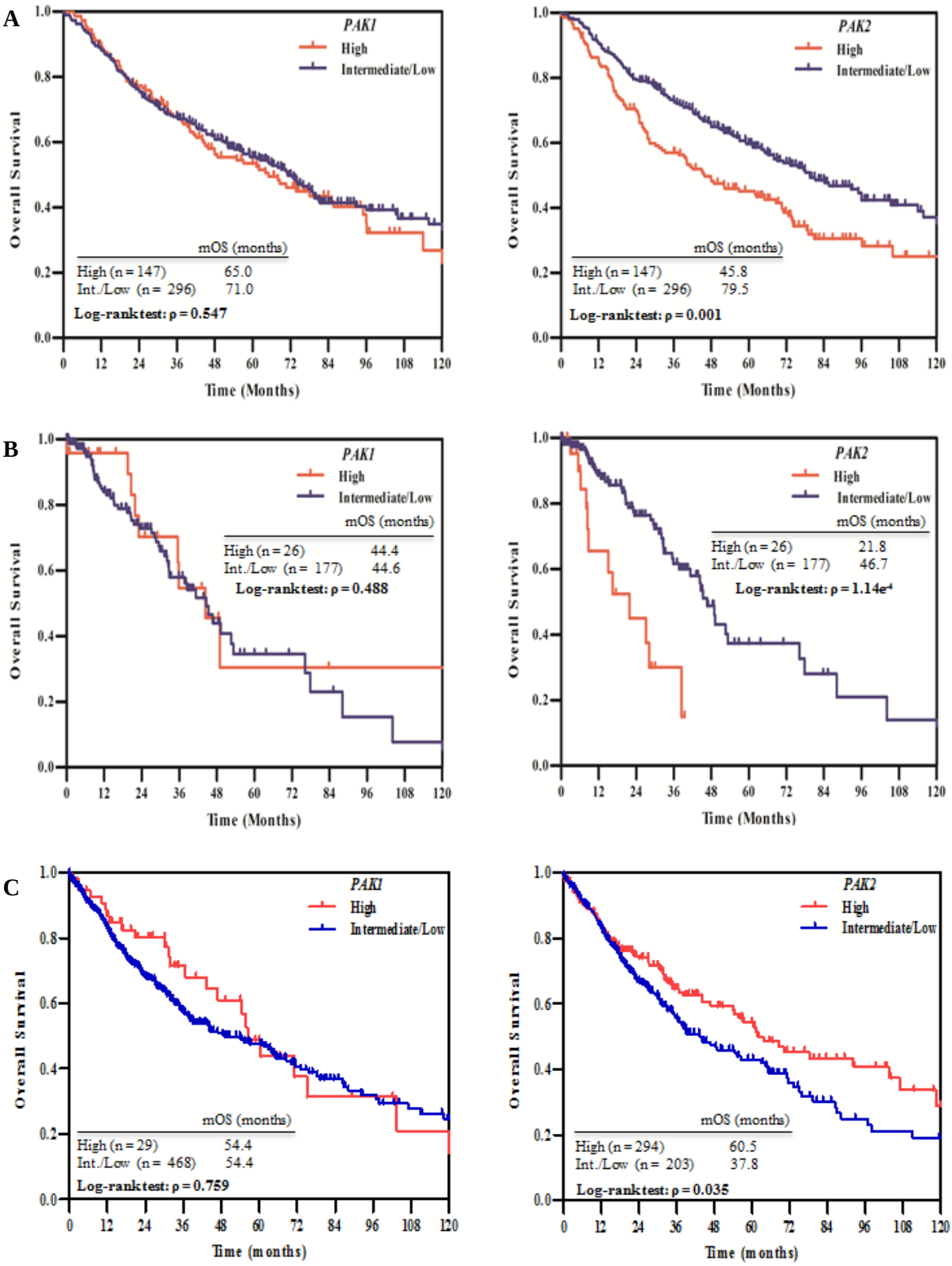
A
PAK1
High
Intermediate/Low
Overall Survival
mOS (months)
High (n = 147) 65.0
Int./Low (n = 296) 71.0
Log-rank test: ρ = 0.547
Time (Months)
PAK2
High
Intermediate/Low
Overall Survival
mOS (months)
High (n = 147) 45.8
Int./Low (n = 296) 79.5
Log-rank test: ρ = 0.001
Time (Months)
B
PAK1
High
Intermediate/Low
Overall Survival
mOS (months)
High (n = 26) 44.4
Int./Low (n = 177) 44.6
Log-rank test: ρ = 0.488
Time (Months)
PAK2
High
Intermediate/Low
Overall Survival
mOS (months)
High (n = 26) 21.8
Int./Low (n = 177) 46.7
Log-rank test: ρ = 1.14e-4
Time (Months)
C
PAK1
High
Intermediate/Low
Overall Survival
mOS (months)
High (n = 29) 54.4
Int./Low (n = 468) 54.4
Log-rank test: ρ = 0.759
Time (months)
PAK2
High
Intermediate/Low
Overall Survival
mOS (months)
High (n = 294) 60.5
Int./Low (n = 203) 37.8
Log-rank test: ρ = 0.035
Time (months)

Figure 2. *PAK1* and *PAK2* Expression Status as Prognostic Indicators in Lung Adenocarcinoma, Stages I-III.

A, Patient clinical data was mined from the Director's Challenge Consortium for the Molecular Classification of Lung Adenocarcinoma (n = 443) and used to estimate survival outcomes based on microarray expression values for *PAK1* (Left) and *PAK2* (Right). Patients were classified as *PAK2/PAK1* high or *PAK2/PAK1* intermediate/low based on tertile analysis of Log_2 transformed microarray values. Log-rank statistics and Kaplan-Meier curves were generated from SPSS software application.

B, Patient clinical data was accessed through cBioPortal Web Application (Lung Adenocarcinoma, Nature 2014). mRNA expression and copy number analysis values were used to define *PAK1* (Left, n = 203) and *PAK2* (Right, n = 203) over-expression groups. For each gene, samples were classified as high or intermediate/low, and Kaplan-Meier survival curves generated using GraphPad Prism 5 including the Log-rank statistics.

C, Patient clinical data was accessed through cBioPortal Web Application (Lung Squamous Cell Carcinoma, Provisional). mRNA expression and copy number analysis values were used to define *PAK1* (Left, n = 497) and *PAK2* (Right, n = 497) over-expression groups. For each gene, samples were classified as high or intermediate/low, and Kaplan-Meier survival curves generated using GraphPad Prism 5 including the Log-rank statistics.

TABLE 1. Univariate Kaplan-Meier Analysis for Overall Survival in Patients from Director's Challenge Lung Consortium Study

Characteristic	***No. of Patients (%)***	***mOS (95% CI)***	***P Value (Log-rank)***
Age			0.015
< 65	214 (48.3)	74.0 months (55.5 – 92.5)	
≥ 65	229 (51.7)	61.2 months (46.3 – 76.1)	
Gender			0.012
Male	223 (50.3)	62.3 months (47.2 – 77.4)	
Female	220 (49.7)	85.6 months (65.3 – 106.0)	
Adjuvant Chemotherapy			0.001
Yes	89 (20.2)	51.0 months (34.1 – 67.9)	
No	351 (79.8)	74.2 months (59.2 – 89.2)	
Adjuvant Radiation			< 0.001
Yes	65 (14.8)	41.0 months (24.4 – 57.6)	
No	374 (85.2)	74.2 months (64.3 – 84.1)	
TNM Stage			< 0.001
Stage I	276 (62.7)	105.4 months (74.4 – 136.4)	
Stage II	95 (21.6)	42.2 months (23.1 – 61.2)	
Stage III	69 (15.7)	21.0 months (12.6 – 29.4)	
PAK2			0.001
High	147 (33.2)	45.8 months (29.3 – 62.3)	
Intermediate/Low	296 (66.8)	79.5 months (61.9 – 97.2)	
PAK1			0.547
High	147 (33.2)	65.0 months (44.1 – 85.9)	
Intermediate/Low	296 (66.8)	71.0 months (59.7 – 82.3)	

Abbreviations: mOS, median Overall Survival; 95% CI, 95% Confidence Interval.

Table 1. Univariate Kaplan-Meier Analysis for Overall Survival in Patients from Director's Challenge Lung Consortium Study
Data generated from SPSS Software application. Patients with unknown clinical covariates were removed prior to running the analysis: staging information (n =3); adjuvant chemotherapy (n = 3); and adjuvant radiation therapy (n = 3).

To validate the findings from the Director's Challenge, we accessed the TCGA lung adenocarcinoma dataset (n = 203) using the cBioPortal web application [78-80]. *PAK1* and *PAK2* were each overexpressed in 13% of patient tumors. Patients with *PAK2* high-expressing tumors exhibited a significant reduction in mOS compared to the intermediate/low expressing group (21.8 vs 46.7 months, Log-rank $\rho = 1.14e^{-4}$), whereas, high *PAK1* expression resulted in no changes to patient survival (44.4 vs 44.6 months, Log-rank $\rho = 0.488$) (Figure 1B). Since publication in 2014, the TCGA lung adenocarcinoma cohort has expanded to 515patients. Again,

TABLE 2. Multivariate Cox Regression Analysis for Overall Survival in Patients from Director's Challenge Lung Consortium Study (N = 435)

Characteristic	***HR (95% CI)***	***P Value***
Age (Continuous)	1.032 (1.018 – 1.047)	< 0.001
Gender		
Male	1.432 (1.094 – 1.875)	0.009
Female (ref.)	1.000	
Adjuvant Chemotherapy		
Yes	1.347 (0.907 – 1.999)	0.139
No (ref.)	1.000	
Adjuvant Radiation		
Yes	1.311 (0.854 – 2.012)	0.216
No (ref.)	1.000	
TNM Stage		
Stage I (ref.)	1.000	
Stage II	2.204 (1.599 – 3.038)	< 0.001
Stage III	3.778 (2.669 – 5.348)	< 0.001
PAK2 (Continuous)	1.540 (1.150 – 2.062)	0.004

Abbreviations: N, number of samples; HR, Hazard Ratio; 95% CI, 95% Confidence Interval.

Table 2: Multivariate Cox Regression Analysis for Overall Survival in Patients from Director's Challenge Lung Consortium Study
Data generated from SPSS Software application. Multivariate Cox Regression analysis was used for the multivariable report. Only clinical covariates found to be significant under a Kaplan-Meier univariate analysis were used as inputs for the multivariate testing. Eight cases from the total cohort of 443 samples were removed from multivariate analysis due to missing values.

PAK2 overexpression significantly correlated with worse clinical outcomes (32.4 vs 52.6 months, Log-rank $\rho = 7.12e^{-4}$). Following these overall survival analyses, we observed a strong negative prognostic effect associated with high *PAK2* mRNA expression in patients with lung adenocarcinoma.

From our research group's initial findings showing increased PAK2 expression in pooled samples of stage I squamous cell carcinoma tumors compared to pooled samples of normal lung tissue, we sought to assess the relationship between *PAK2* expression and patient outcome in the publically available TCGA lung squamous cell carcinoma provisional cohort [20]. Using the same cut-offs for high or intermediate/low expression from the lung adenocarcinoma cohort, high *PAK2* expression led to increased mOS versus the

intermediate/low expression group (60.5 vs. 37.8 months, Log-rank $\rho = 0.035$)(Figure 1B). Additionally, there was an increase in the percentage of patients with high *PAK2* expression in lung squamous cell carcinoma, 59%, compared with 13% of the lung adenocarcinoma population. The increase in the presence of *PAK2* overexpression in squamous cell carcinoma is primarily due to chromosome 3q focal amplification where *PAK2* resides. Similar to the lung adenocarcinoma cohort, *PAK1* expression did not impact survival outcomes (54.4 vs. 54.4 months, Log-rank $\rho = 0.759$). These results further exemplify how the two main sub-types of NSCLC are different diseases, and PAK2 may function differently between lung squamous cell carcinoma and adenocarcinoma.

PAK1, PAK2 and phospho-PAK1 (Ser^{144})/PAK2 (Ser^{141}) Exhibit Differential Patterns of Expression across a Wide Panel of NSCLC Cell Lines

To study the effects of PAK1 and PAK2 *in* vitro, we first assessed the protein expression profile of endogenous PAK1, PAK2, and phosphorylated PAK1 (Ser^{144})/PAK2 (Ser^{141}) across 31 established NSCLC and three immortalized bronchial epithelial cell lines, 16HBE, HBEC-3KT, and HBEC-3KTR (Fig. 3A). PAK1 exhibited a less frequent pattern of expression compared to PAK2. PAK2 was detected in 28 of the 31 lung cancer cell lines at variable intensities, and in all three of the immortalized bronchial epithelial cells. Most notably, we detected a higher level of activated PAK1/PAK2 protein expression in lung cancer cell lines compared to immortalized bronchial epithelial cells, suggesting increased functional PAK1/2 in the tumor setting. Of the 31 cancer samples, we detected phosphorylated PAK1 (Ser^{144})/PAK2 (Ser^{141}) in 22 of the cell lines.

Using a broad spectrum of NSCLC cell lines with known genotypes, we evaluated if there was a correlative relationship between PAK1/2 activation and the NSCLC driver oncogenes *EGFR* and *KRAS*. There was no difference in the percentage of phospho-PAK1/2 positive cell lines based on *EGFR* genotype status. However, there was a negative association between phosphorylated PAK1/2 and mutant *KRAS* (Fisher's exact test, $\rho = 0.001$). Among 10 *KRAS* mutant cell lines, only 3 expressed phospho-PAK1/2, whereas 90% of *KRAS*

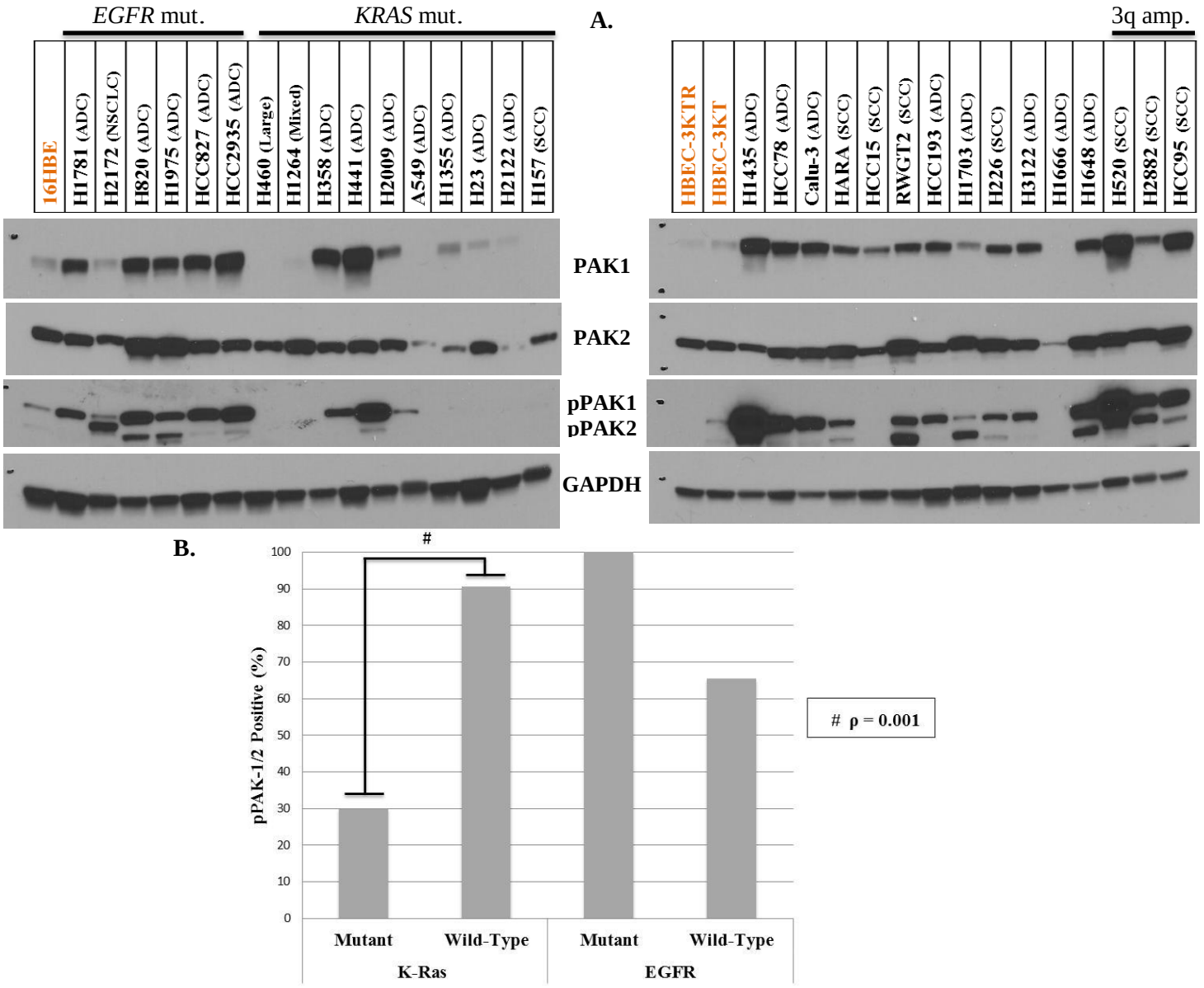

Figure 3. Variable expression pattern of activated PAK1/PAK2 across 31 NSCLC Cell Lines.

A, Protein extracts were run on 10% SDS-PAGE pre-cast gels to detect relative expression levels of endogenous PAK1, PAK2, and phospho-PAK1 (Ser^{144})/PAK2 (Ser^{141}). GAPDH was probed for as a loading control. These images illustrate the heterogeneity of phospho-PAK1/2 and PAK1 protein expression, and more importantly, an increased level of expression in the disease model compared to immortalized human bronchial epithelial cells (red font). Known genetic and chromosomal alterations are listed above each cell line.

B, Graphical illustration of the relationship between phospho-PAK1 (Ser^{144})/phospho-PAK2 (Ser^{141}) and co-expression with activating mutations in NSCLC driver oncogenes, *EGFR* and *KRAS*. There was a negative association discovered between the presence of phosphorylated PAK1/2 and mutant *KRAS* expression (Fisher's Exact test, $\rho = 0.001$). No positive or negative correlations could be inferred between *EGFR* mutation status and activated PAK1/2 levels; however, there is a trend towards increased phospho-PAK1/2 levels in cell lines with activating *EGFR* mutations.

wild-type samples exhibited active PAK1/2 (Fig. 3B). Furthermore, the presence of activated PAK was absent in HBEC-3KTR cells, which uniquely express *KRAS*^{G12V}, compared to their parental HBEC-3KT cells that express wild-type *KRAS* (Fig. 3A). In support of these findings, reverse phase protein array (RPPA) data from the TCGA lung adenocarcinoma dataset illustrated decreased phosphorylation events associated with KRAS signaling in a cohort of patient samples with upregulated *PAK2* expression, including reduced ERK1/2 (pT202) and STAT3 (pY705) expression levels (Table 3).

		Mean Protein Expression		SD of Protein Expression			
Gene	Cytoband	PAK2 High	PAK2 Intermediate/Low	PAK2 High	PAK2 Intermediate/Low	p-Value	q-Value
NAPSA	19q13.33	-0.14	0.17	0.25	0.66	4.88E-10	1.14E-07
PGR	11q22.1	-0.07	0.08	0.16	0.25	9.01E-08	1.06E-05
ESR1_PS118	6q25.1	-0.07	0.06	0.17	0.26	1.02E-05	4.28E-04
NKX2-1	14q13.3	-1.5	-0.08	2.17	1.26	4.72E-05	1.46E-03
ESR1	6q25.1-q25.2	-0.05	0.13	0.31	0.5	8.19E-04	0.0128
NRAS	1p13.2	-0.08	-0.01	0.14	0.15	1.01E-03	0.0139
SNAI1	20q13.13	0.04	0.29	0.42	1.06	4.95E-03	0.0453
MET	7q31.2	0.04	0.26	0.39	0.97	5.72E-03	0.048
MTOR_PS2448	1p36.2	-0.15	-0.01	0.31	0.31	5.74E-03	0.048
PECAM1	17q23.3	-0.09	0.05	0.32	0.34	7.38E-03	0.0575
FOXO3_PS318_S321	6q21	-0.06	0.01	0.17	0.18	8.62E-03	0.0609
RPS6KB1_PT389	17q23.1	-0.04	0.07	0.27	0.27	9.87E-03	0.0642
AR	Xq12	-0.05	0.04	0.22	0.26	0.012	0.0737
MAPK1_PT202_Y204	22q11.21	-0.15	0.08	0.62	0.61	0.0171	0.0954
MAPK3_PT202_Y204	16p11.2	-0.15	0.08	0.62	0.61	0.0171	0.0954
CLDN7	17p13.1	-0.07	0.24	0.8	0.94	0.0179	0.0954
CAV1	7q31.2	-0.32	0.14	1.22	1.16	0.0194	0.0954
ERBB3	12q13.2	-0.08	0.09	0.43	0.46	0.0196	0.0954
PDK1_PS241	2q31.1	-0.13	-0.03	0.29	0.29	0.0219	0.1
PDCD4	10q25.2	-0.22	0.03	0.71	0.66	0.0248	0.111
STAT3_PY705	17q21.31	-0.19	-0.02	0.49	0.42	0.0262	0.114
PRKCD_PS664	3p21.31	-0.03	0.03	0.15	0.19	0.0369	0.142
RICTOR	5p13.1	-0.23	0	0.7	0.7	0.0454	0.165

Table 3: Reduced total protein and phosphorylation events in high *PAK2* lung adenocarcinoma tumor samples compared to intermediate/low *PAK2* expressing tumor samples. High *PAK2* expression was observed in 71 patient samples (13.6%) of the cohort (n = 522). Data was retrieved from cBioPortal Web Application on January 30,2018.

Combining our phosphorylation protein data from the 31 NSCLC cell lines with microarray RNA gene expression and copy number analysis from the Cancer Cell Line Encyclopedia (CCLE), we identified a strong correlative association between detectable phosphorylated PAK1/2 and *PAK2* mRNA expression. 24 cell lines

Gene	Cytoband	Mean Protein Expression		SD of Protein Expression		p-Value	q-Value
		KRAS MUT/ NF1 MUT	KRAS WT/ NF1 WT	KRAS MUT/ NF1 MUT	KRAS WT/ NF1 WT		
MAP2K1_PS217_S221	15q22.1-q22.33	0.26	0.02	0.42	0.29	1.22E-05	2.86E-03
MAPK1_PT202_Y204	22q11.21	0.31	-0.02	0.7	0.58	2.52E-04	0.0147
MAPK3_PT202_Y204	16p11.2	0.31	-0.02	0.7	0.58	2.52E-04	0.0147
RPS6_PS235_S236	9p21	0.3	0	0.72	0.67	1.29E-03	0.034
YBX1_PS102	1p34	0.16	0.01	0.35	0.3	1.43E-03	0.034
MTOR_PS2448	1p36.2	0.07	-0.06	0.31	0.31	2.28E-03	0.0381
COL6A1	21q22.3	0.33	0.1	0.63	0.49	3.14E-03	0.049
PECAM1	17q23.3	0.15	0	0.43	0.3	4.34E-03	0.0635
PDCD4	10q25.2	0.21	-0.06	0.76	0.64	5.21E-03	0.0717
PXN	12q24.23	0.03	-0.16	0.52	0.55	5.86E-03	0.0762
CLDN7	17p13.1	0.45	0.13	0.93	0.92	8.73E-03	0.105
KIT	4q12	0.46	0.17	0.88	0.75	0.0102	0.114
CAV1	7q31.2	0.41	-0.01	1.42	1.09	0.0181	0.169
STAT3_PY705	17q21.31	0.05	-0.07	0.39	0.44	0.0207	0.184
SRC	20q11.23	0.12	0.01	0.38	0.3	0.0216	0.184
RPS6_PS240_S244	9p21	0.29	0.02	0.92	0.8	0.022	0.184
NAPSA	19q13.33	0.25	0.09	0.53	0.67	0.023	0.186
CDH1	16q22.1	0.04	-0.14	0.63	0.77	0.0339	0.22
PARP1	1q42.12	0.14	0.02	0.48	0.32	0.0388	0.245
ERBB3	12q13.2	0.16	0.04	0.47	0.45	0.0506	0.282

Table 4: Upregulated total protein and phosphorylation events in *KRAS* or *NF1* mutant lung adenocarcinoma tumor samples compared to wild-type expressing tumor samples. The mutations were mutually exclusive, aside from one tumor sample that contained a mutation in each of the two selected genes. There were 75 KRAS mutant and 27 mutant NF1 tumor samples, with one patient sample having overlapping mutations (n = 520). Data was retrieved from cBioPortal Web Application on January 30,2018.

were shared between our *in vitro* analysis and the CCLE. Ranking the cell lines by their respective *PAK1* or *PAK2* expression values, the cell lines with basal levels of activated PAK1/2 clustered to the top of a ranked list. Using the point-biserial correlation equation, we observed a strong correlative trend between *PAK2* expression and detectable phosphorylated PAK1 (Ser^{144})/PAK2 (Ser^{141}) ($r^2 = 0.769$, $\rho = 1.13e^{-5}$) (Fig. 4A, B right panels). The same analysis with *PAK1* demonstrated a difference in the mean mRNA expression between the phospho-PAK(+) and phospho-PAK(-) cell lines, but the correlation coefficient was low (Fig. 4A, B left panels). These results along with the *in silico* clinical outcome studies associated with *PAK2* mRNA expression in lung cancer patients, suggest a functional role for PAK2 in lung tumor biology.

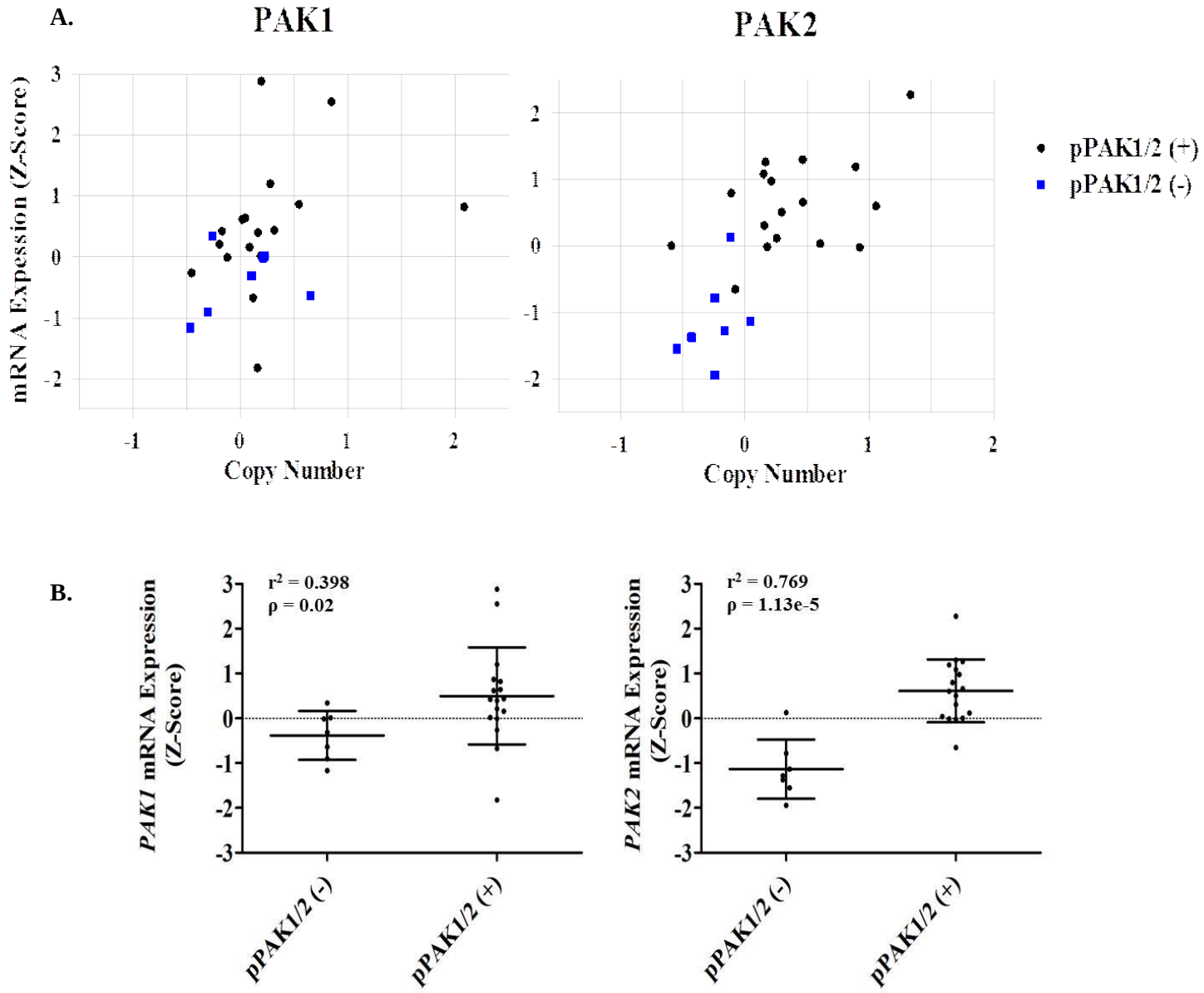

Figure 4. Positive Correlation Between Activated PAK1/PAK2 and Genomic and Transcriptomic *PAK2* Expression Levels

A, Scatter plots illustrating the correlative relationship between phospho-PAK1 (Ser^{144})/PAK2 (Ser^{141}) and the DNA copy number values and mRNA expression levels of *PAK1* (left) and *PAK2* (right). We observed a clear separation between phospho-PAK1/2 (+) or (-) cell lines when plotting *PAK2* gene copy number by mRNA expression. DNA copy number and mRNA expression values were downloaded from cBioPortal web application.

B, Box and Whisker plots visualizing the differences between phospho-PAK1 (Ser^{144})/PAK2 (Ser^{141}) protein expression levels and the mRNA expression levels of *PAK1* (left) and *PAK2* (right). The point-biserial correlation coefficient was used to statistically assess the relationship between phospho-PAK1 (Ser^{144})/PAK2 (Ser^{141}) and either *PAK1* or *PAK2* mRNA expression in NSCLC cell lines. An unpaired student's T-test was then used to measure the significance of the correlation. All graphs were generated using GraphPad Prism 5.

Phospho-PAK1/2 Expression Correlates to PAK2 Dependent Cell Motility

In our initial functional studies, we investigated how PAK2 silencing affects cell motility in samples with and without basal phosphorylated PAK1/2 using a transwell cell migration assay. We selected H1703 and H2882 cell lines representing phospho-PAK1/2 positive samples, as well as non-phosphorylated PAK1 (Ser^{144})/PAK2 (Ser^{141}) cell lines A549 and H157. In the H2882 and H1703 samples, both *PAK2* shRNA constructs reduced cell migration 40-60% versus non-target controls (Fig. 5A, B). In the cell lines lacking phospho-PAK1/2 expression, neither cell line exhibited a significant reduction in cell motility following PAK2 loss (Fig. 6A, B). For the A549 cells, we actually observed a small increased in cell motility using one of the PAK2 shRNA constructs. These findings highlighted a role for PAK2 promoting cell motility specifically in NSCLC samples with basal levels of activated PAK1/2.

Both Pharmacological and Genetic Inhibition of PAK2 Disrupts Wound-Healing in NSCLC phospho-PAK1/2 Expressing Cells

To further probe PAK2-dependent NSCLC cell motility, H2882 phospho-PAK1/2 positive cells were analyzed for wound-healing. Silencing *PAK2* impaired wound closure by 30-40%, supporting the findings from the earlier transwell cell migration experiment (Fig. 7A, B). In addition to gene knockdown, the ATP mimetic PAK inhibitor, PF-3758309, was employed to block PAK-dependent kinase function.[83] A dose-dependent response was observed with increasing concentrations of drug in cells with intact PAK2 signaling, starting at 1 and 10 nM concentrations (Fig. 7C). However, there was only a limited additional benefit when combining both PF-3758309 and *PAK2* gene silencing, indicating a reliance on *PAK2* expression for H2882 PAK-dependent cell motility. In the shPAK2 #1 infected H2882 cells, there was no observed difference in wound-healing ability between vehicle alone and any of the four doses of drug. With shPAK2 #2, a significant decrease in wound-healing only occurred at the 100 nM drug concentration, and the reduction was marginalized compared to the effect observed in *PAK2*-expressing cells. Our results suggest phospho-PAK1/2 expressing cells require functional PAK2 kinase to promote their full cell motility potential.

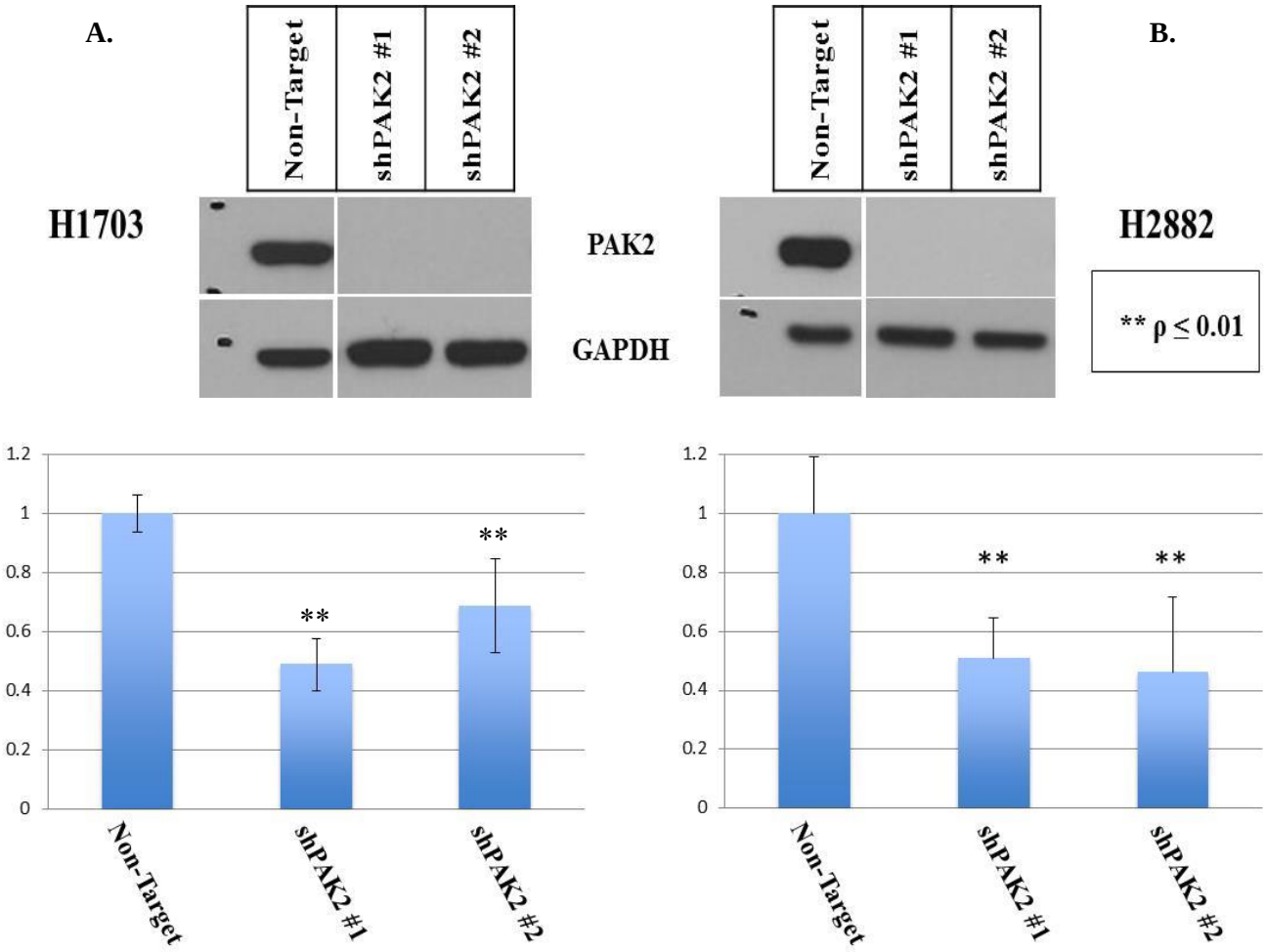

Figure 5. Phospho-PAK1/2 Expression Correlates to PAK2-Dependent Cell Motility in NSCLC

A and B, Western blot images illustrating targeted knockdown of PAK2 in two cell lines expressing phosphorylated PAK1 (Ser^{144})/PAK2 (Ser^{141}), H1703 (left panel, A) and H2882 cells (right panel, B). On the bottom are graphical representations of three independent transwell migration assays performed in each cell line. In both cell lines, efficient stable knockdown of PAK2 protein expression effectively inhibited cell migration using each shRNA targeting construct (Unpaired student's t-test, $\rho < 0.01$). Each value represents the mean ± s.d.

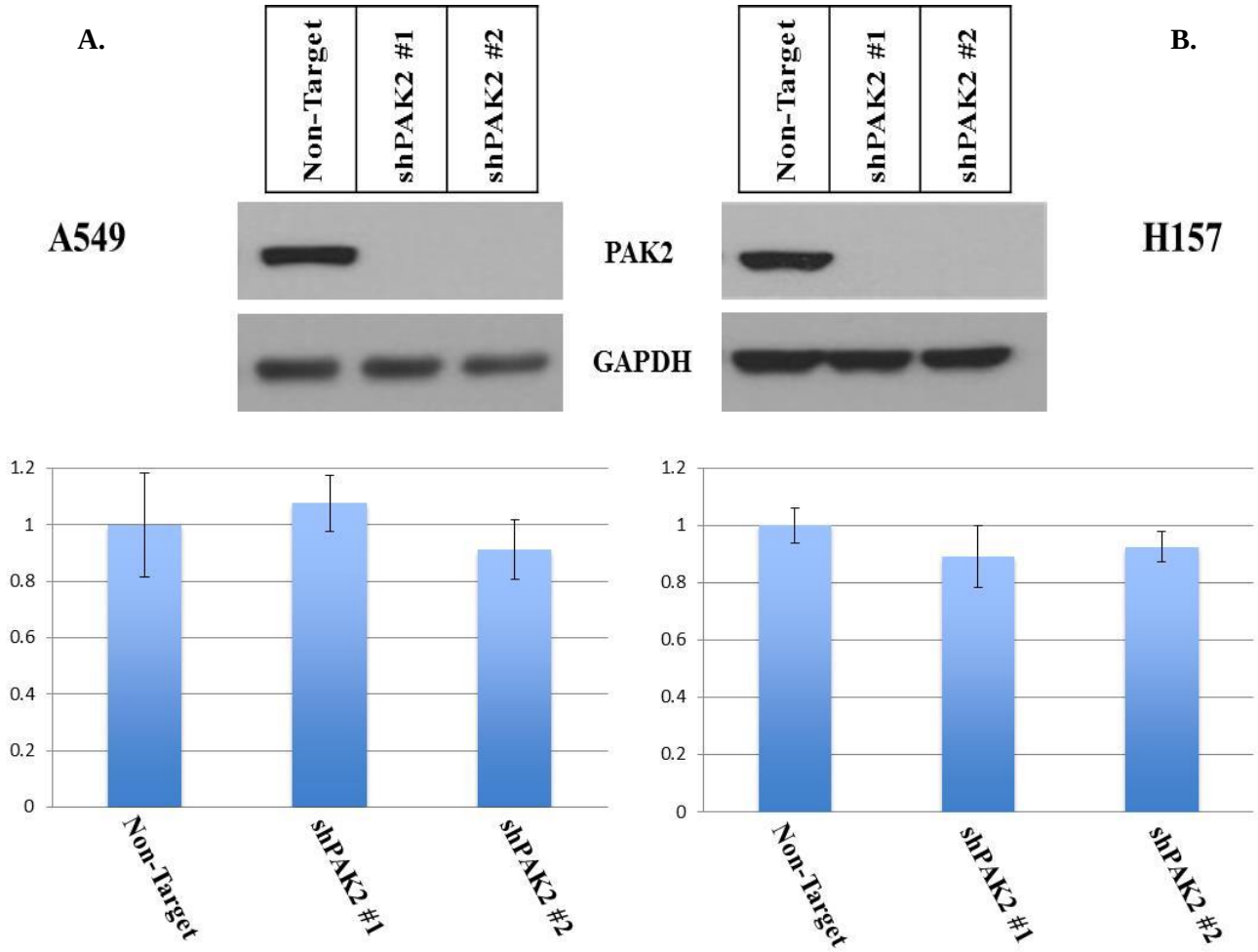

Figure 6. Silencing PAK2 Expression in NSCLC Cells Lacking Basal Levels of Phosphorylated-PAK1 (Ser^{144})/PAK2 (Ser^{141}) Does Not Alter Cell Migration Potential

A and B, Western blot images of targeted knockdown of PAK2 in two cell lines negative for endogenous phosphorylated-PAK1(Ser^{144})/PAK2 (Ser^{141}), A549 (left panel, A) and H157 cells (right panel, B). On the bottom are graphical representations of three independent transwell migration assays performed in each cell line. In both cell lines, knockdown of PAK2 protein expression did not impede cell migration compared to the non-target control. Each value represents the mean ± s.d.

A.

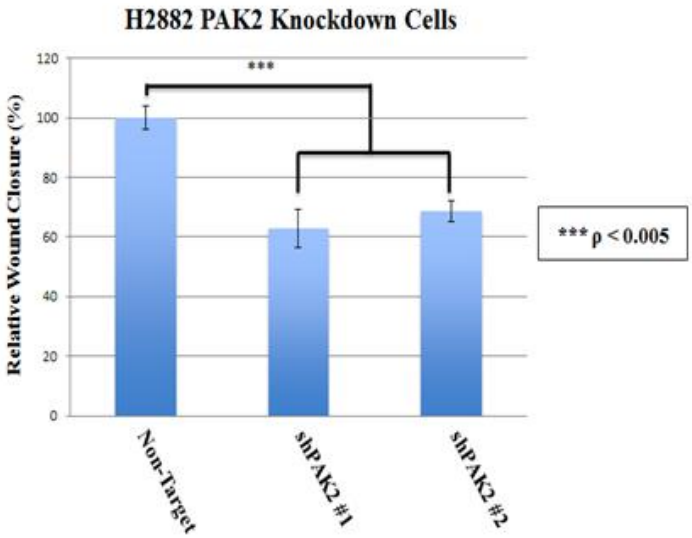
H2882 PAK2 Knockdown Cells
Relative Wound Closure (%)
120
100
80
60
40
20
0
***
*** ρ < 0.005
Non-Target
shPAK2 #1
shPAK2 #2

B.

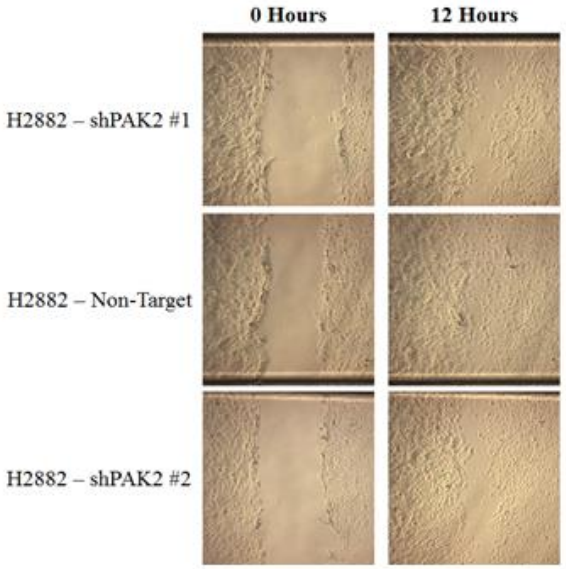
0 Hours
12 Hours
H2882 – shPAK2 #1
H2882 – Non-Target
H2882 – shPAK2 #2

C.

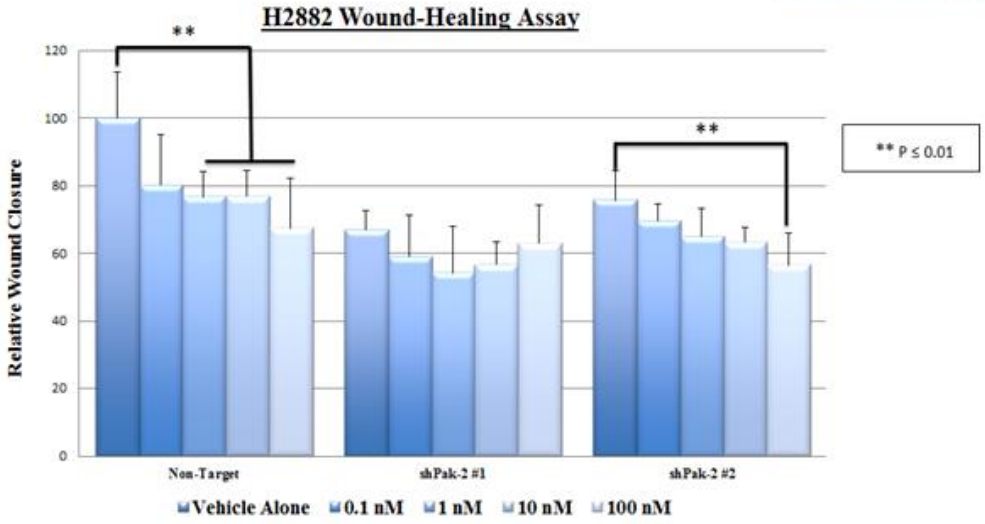
H2882 Wound-Healing Assay
Relative Wound Closure
120
100
80
60
40
20
0
**
**
** P ≤ 0.01
Non-Target
shPak-2 #1
shPak-2 #2
Vehicle Alone
0.1 nM
1 nM
10 nM
100 nM

D.

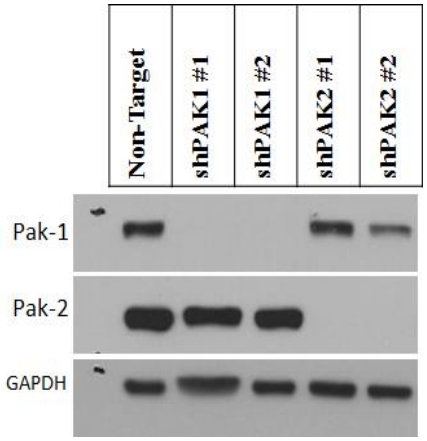
Non-Target
shPAK1 #1
shPAK1 #2
shPAK2 #1
shPAK2 #2
Pak-1
Pak-2
GAPDH

E.

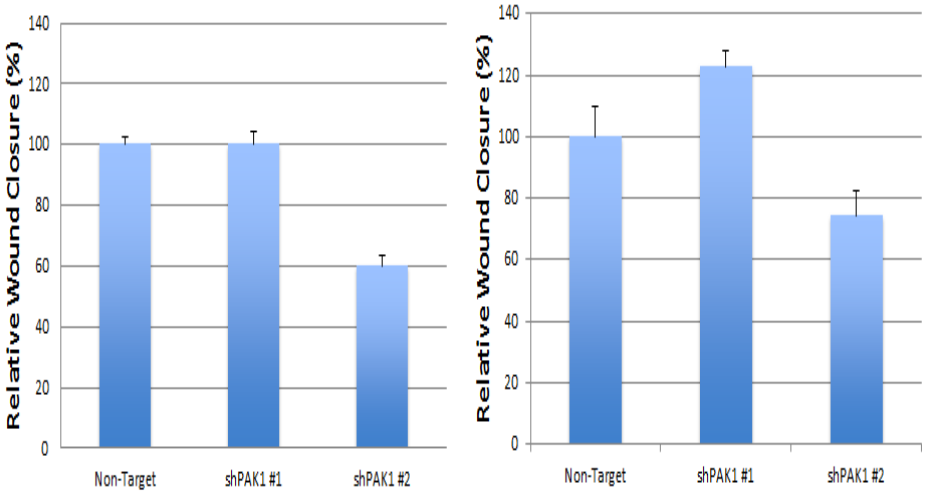
Relative Wound Closure (%)
140
120
100
80
60
40
20
0
Non-Target
shPAK1 #1
shPAK1 #2
Relative Wound Closure (%)
140
120
100
80
60
40
20
0
Non-Target
shPAK1 #1
shPAK1 #2

Figure 7. Both Pharmacological and Genetic Inhibition of PAK2 Disrupts Cell Motility in NSCLC pPAK1/2 Expressing Cells.
A, Wound-healing assay using shRNA knockdown of PAK2. Both shRNA constructs targeting PAK2 effectively inhibit cell migration as assessed by wound-healing capacity in phospho-PAK1/2 positive H2882 cells ($p < 0.005$).
B, Representative images from the initial and final timepoints in non-target (middle), and two PAK2 knockdown constructs (shPAK2 #1, top; shPAK2 #2, bottom). The duration of the study was 12 hours. Images were taken on a Nikon Eclipse TE2000-U microscope at 4X magnification. Images were analyzed following acquisition using ImageJ software analysis tools.
C, Wound-healing assay, combined inhibition of PAK signaling using both shRNA gene knockdown and the pan-PAK inhibitor, PF-3758309. Observed consistent inhibition of migration in cell populations with intact PAK2 protein expression, with dose dependent effects demonstrated in non-target control cells at 1, 10 and 100 nM concentrations of drug ($p < 0.01$). In the two PAK2 knockdown constructs, little change is observed between vehicle alone and drug treated cells, except in the second knockdown construct, and at the highest dose of drug investigated ($p < 0.01$).
D, Western blot images illustrating targeted PAK1 knockdown using two unique shRNA constructs with no effect on PAK2 protein expression in the H2882 cell line.
E, Wound-healing assay with stable PAK1 knockdown in phosphorylated-PAK1 (Ser^{144})/PAK2 (Ser^{141}) positive H2882 cells. Both shRNA constructs demonstrate equivalent knockdown efficiencies of PAK1 protein, but show disparate effects on cell motility in two separate assays.

To confirm our thoughts suggesting a greater reliance on PAK2 than on PAK1 for regulating cell motility in phospho-PAK1/2 expressing NSCLC cells, PAK1 protein expression was silenced in H2882 cells (Fig. 7D). PAK1 protein expression was abrogated using two shRNA constructs, but their effects on wound-healing were varied. On average, the first construct, shPAK1 #1, increased H2882 wound closure, whereas shPAK1 #2 infected cells decreased wound-healing function by 30% (Fig. 7E). Since the findings are inconsistent between the two shRNA constructs, we cannot confidently report PAK1 controls cell migration in H2882 cells. Overall, these results, including the dual genetic and pharmacological inhibition study, point to a stronger dependency on PAK2 kinase expression in promoting cell motility compared to PAK1 within the subset of phospho-PAK1/2 positive NSCLC cells.

PAK Inhibition Differentially Affects NSCLC Three-Dimensional Cell Migration

To investigate NSCLC cell motility in a three-dimensional setting, A549, H1703, and H2882 cell

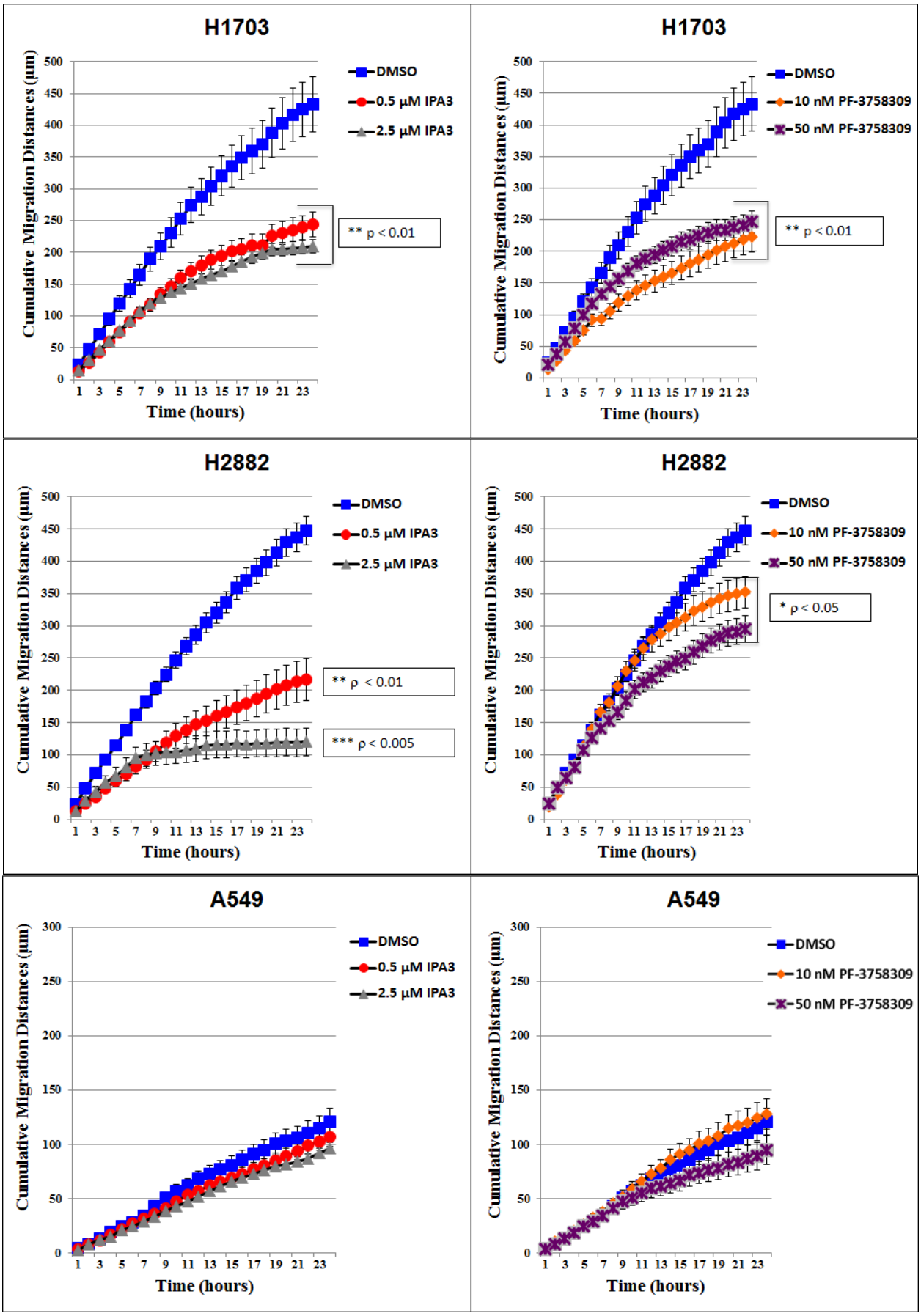
H1703
Cumulative Migration Distances (µm)
Time (hours)
DMSO
0.5 µM IPA3
2.5 µM IPA3
** p < 0.01
H1703
Cumulative Migration Distances (µm)
Time (hours)
DMSO
10 nM PF-3758309
50 nM PF-3758309
** p < 0.01
H2882
Cumulative Migration Distances (µm)
Time (hours)
DMSO
0.5 µM IPA3
2.5 µM IPA3
** ρ < 0.01
*** ρ < 0.005
H2882
Cumulative Migration Distances (µm)
Time (hours)
DMSO
10 nM PF-3758309
50 nM PF-3758309
* ρ < 0.05
A549
Cumulative Migration Distances (µm)
Time (hours)
DMSO
0.5 µM IPA3
2.5 µM IPA3
A549
Cumulative Migration Distances (µm)
Time (hours)
DMSO
10 nM PF-3758309
50 nM PF-3758309

Figure 8. Pharmacological PAK Inhibition Differentially Effects NSCLC Three-Dimensional Cell Motility.
NSCLC cell lines, H1703 (Top Panel), H2882 (Middle Panel), and A549 (Bottom Panel), were cultured in 24-well plates containing three-dimensional aligned nanofibers and visualized using time-lapse confocal microscopy for 24 hours. Two pharmacological inhibitors of PAK kinase activity, IPA-3 (Left Panels, DMSO, 0.5, and 2.5 uM) and PF-3758309 (Right Panel, DMSO, 10, and 50 nM) were added to the cells. Confocal microscope (Olympus IX73) images using a 10x objective and fluorescence excitation/emission wavelengths of 480/520 nm were taken from three distinct regions per well every 30 minutes over a 24 hour period. Utilization of the MTrackJ cell migration tracking software plugin for ImageJ, 25 cells per video were selected and their displacement vectors tracked and recorded with respect to time. The average total migration distance was reported with standard deviations for each of the NSCLC cell lines. In each cell line model, the cumulative migration distance endpoint values between treated and untreated samples were compared to one another using the Tukey's Test statistic (MiniTab 16). * $\rho < 0.05$, ** $\rho < 0.01$, and *** $\rho < 0.005$.

migration potential was evaluated on aligned nanofiber substrates closely mimicking the fibrillar extracellular matrix of the tumor microenvironment. Phospho-PAK1/2 expressing cell lines, H1703 and H2882, migrated cumulative distances of 433 and 447 μm, respectively, whereas the A549 cells lacking phospho-PAK1/2 migrated 121 μm (Fig. 8). When exposed to IPA-3 or PF-3758309, cell movement along the nanofibers was significantly reduced in both H1703 and H2882 cells (Fig. 8, top and middle panels). Total cell migration diminished approximately 50% of the DMSO control with each of the PAK inhibitors in H1703 cells (Fig. 8, top panel, $\rho < 0.01$). However, H2882 cells showed differential sensitivities to each of the PAK inhibitors. A dose response to IPA-3 was observed in H2882 cells, with reductions of 52% and 73% at 0.5 and 2.5 μM, respectively (Fig. 8, middle panel, left). The ATP-mimetic compound, PF-3758309, diminished cell migration in H2882 cells, but not as strongly as IPA-3, with decreases of 22% and 34% at each dose of drug (Fig. 8, middle panel, right). Conversely, when treating phospho-PAK1/2 negative cells, A549, there were no observed changes to migration potential upon PAK inhibition (Fig. 8, bottom panel). Cumulative distances of 121, 107, and 97 μm were measured in the DMSO, 0.5 μM, and 2.5 μM IPA-3 treated cells, and similar findings were observed at each PF-3758309 dose. Our results from tracking individual cells on aligned nanofibers strongly support the claim that PAK inhibition effectively curbs cell migration in NSCLC cell lines with basal levels of activated PAK1/2 expression.

Discussion

Cancer cell motility is fundamental to tumor cell dissemination and metastasis. In NSCLC, tumor recurrence and metastasis are leading factors associated with disease-related death, making the identification of novel prognostic markers for aggressive tumors a critical area of research. Prior studies have shown PAK overexpression to be tightly associated with disease progression and metastasis in various tumor settings, but the role of PAK2 in NSCLC is less well-established [7, 9, 12, 84]. Using publically available databases integrating patient survival and RNA expression data, we show PAK2 to be a promising prognostic biomarker candidate for lung adenocarcinoma. *In vitro g*enetic and pharmacological inhibition of PAK1 and PAK2 was employed to assess their respective functions in NSCLC cell migration using both expected and novel experimental methods.

In an earlier study, our research group identified both PAK1 and PAK2 to be upregulated in NSCLC, but no association was observed with patient survival [20]. Most likely, the lack of a prognostic finding resides in the lower patient sample sizes, and the design of the study. Kikuchi and colleagues were focusing on differences in protein expression between lung squamous cell carcinoma and adenocarcinoma, as well as changes from normal and tumor lung tissues. With access to larger patient datasets in our current study, we identified a novel relationship between *PAK2* overexpression and poor patient survival in lung adenocarcinoma using two independent datasets. From data gathered in the Director's Challenge Consortium, a multivariate regression analysis identified *PAK2* as an independent prognostic factor regardless of TNM status. Supporting our initial findings, we again observed a strong negative association between high *PAK2* expression levels and patient overall survival in the independent TCGA lung adenocarcinoma patient cohort (Figure 2A,B). *PAK1* overexpression, which is as frequently overexpressed as *PAK2* in the TCGA lung adenocarcinoma cohort is not associated with overall survival. To our knowledge, our finding from the *in silico* clinical analysis is the first report of such an association between poor patient survival and *PAK2* overexpression. In support of our findings, recent studies have observed similar prognostic values with upstream activators of PAKs. Chang and colleagues reported that high *GIT1* expressing tumors significantly correlated with worse clinical outcomes in

cases of lung adenocarcinoma, and not large or squamous cell carcinomas of the lung [72, 73]. Our clinical findings point towards *PAK2* expression being an encouraging prognostic biomarker that could be used for identifying lung adenocarcinoma patients as having a more aggressive disease.

A current literature search finds a cooperative relationship between PAKs and KRAS, and in some cases a requirement for PAK signaling to promote KRAS tumorigenesis [17-19, 22, 24]. However, these reports all focus on PAK1 or PAK4, and as has been shown there are differences in the downstream effectors of the individual PAKs. In our report, we show two novel findings regarding KRAS and PAK2. Our cell line data illustrates an inverse relationship between the presence of activating *KRAS* mutations and the presence of activated PAK1/2 in NSCLC. In support of these *in vitro* results, RPPA data generated from the TCGA lung adenocarcinoma dataset exhibits opposing signaling mechanisms between tumors harboring mutant *KRAS* and high *PAK2* expressing tumors (Tables 3 and 4). *PAK2* overexpressing tumors display an abundance of changes in phosphorylation events linked to KRAS inactivity. The alterations in phosphorylation events are predominantly decreases in pro-growth and survival phosphorylation events. Though these tumors exhibit diminished proliferative signaling, the patients experienced reduced overall survival outcomes. One explanation for this paradoxical observation follows the reciprocal nature of tumor proliferation and migration known as the "go" or "grow" hypothesis[85]. Additionally, it tends to follow the pattern that PAKs play a greater role in cell motility, and thus higher expression and activity would portend to more cell migration and possibly metastasis than tumor cell proliferation.

In addition to the link between *PAK2* overexpression and poor patient outcomes, we also report a rise in basal levels of activated PAK1/2 protein expression across a diverse set of 31 NSCLC cell lines compared to immortalized bronchial epithelial cells. The *in vitro* finding supports earlier studies illustrating elevated expression of upstream p21-activated kinase activators in lung cancer. Due to the previously described cell motility signaling of PAKs, our *in vitro* studies primarily focus on cancer cell migration. We observe a dependence on PAK2 expression for maintaining full cell motility potential in NSCLC samples expressing basal levels of phospho-PAK1 (Ser^{144})/PAK2 (Ser^{141}). Though we do not see a consistent loss of cell motility with

PAK1 gene silencing, contrary to other publications, our pharmacological experiments do support our finding that in our system, PAK2 plays a more prominent role in promoting cell migration [22, 23]. For example, when PAK2 is genetically silenced, the addition of the PAK small molecule inhibitor does not show further loss in cell migration potential. These results point to PAK1 being less involved in cell motility signaling, but further studies are required to better comprehend the different roles PAK1 and PAK2 play across NSCLC sub-types. Coniglio and colleagues reported PAK1 and PAK2 do share many downstream signaling partners, but they adopted differential cellular localization patterns leading to distinct cell motility signaling pathways.[69]

To enhance our cell migration findings, a novel three-dimensional experimental model system was employed a) to better represent cell motility in the tumor microenvironment, b) for enhanced quantitative analysis, and c) improved drug assessment. The processes associated with cell migration and PAK signaling, including filopodia extension and stress fiber formation, are greatly affected by substrate biology [22, 86]. The aligned nanofiber experiments better simulate topography and tumor microenvironment, and thus improve upon the transwell and wound-healing assays. With the use of live cell imaging, we could identify how quickly the inhibitors affected cell motility. We observed that in both phospho-PAK1/2 expressing cell, IPA-3 impedes cell mobility more rapidly than PF-3758309. These benefits enhanced our ability to confidently state our finding that PAK signaling regulates cell motility in cells that express basal levels of activated PAK1 (Ser^{144})/PAK2 (Ser^{141}).

In summary, we show PAK2 to be a frequently overexpressed pro-migratory signaling kinase associated with poor survival in lung adenocarcinoma. The levels of activated PAK1/2 are higher in NSCLC cell lines compared to normal immortalized bronchial epithelial cells. We demonstrate that two unique small molecule inhibitors, PF-3758309 and IPA-3, effectively reduce cell migration in phospho-PAK1/2 expressing cells. Developing a PAK2 specific inhibitor could assist in blocking tumor cell dissemination, and improve upon earlier less specific PAK inhibitors that have failed in the clinic [74, 77]. However, preclinical studies need to be executed to better understand the *in vivo* effects of PAK2 inhibition, in addition to refining how to select which patients would benefit from targeting these tumor cell migration pathways.

WORKS CITED

1. Siegel, R.L., K.D. Miller, and A. Jemal, *Cancer statistics, 2018.* CA Cancer J Clin, 2018. **68**(1): p. 7-30.
2. Ferlay J, S.I., Ervik M, et al. *GLOBOCAN 2012 v1.0, Cancer Incidence and Mortality Worldwide: IARC CancerBase No. 11 [Internet]*. 2013 11/08/2014]; Available from: http://globocan.iarc.fr.
3. Santana-Davila, R., et al., *Cisplatin versus carboplatin-based regimens for the treatment of patients with metastatic lung cancer. An analysis of Veterans Health Administration data.* J Thorac Oncol, 2014. **9**(5): p. 702-9.
4. Schiller, J.H., et al., *Comparison of four chemotherapy regimens for advanced non-small-cell lung cancer.* N Engl J Med, 2002. **346**(2): p. 92-8.
5. Peters, S., et al., *Metastatic non-small-cell lung cancer (NSCLC): ESMO Clinical Practice Guidelines for diagnosis, treatment and follow-up.* Ann Oncol, 2012. **23 Suppl 7**: p. vii56-64.
6. Chaffer, C.L. and R.A. Weinberg, *A perspective on cancer cell metastasis.* Science, 2011. **331**(6024): p. 1559-64.
7. Bokoch, G.M., *Biology of the p21-activated kinases.* Annu Rev Biochem, 2003. **72**: p. 743-81.
8. Zhao, Z.S. and E. Manser, *PAK and other Rho-associated kinases--effectors with surprisingly diverse mechanisms of regulation.* Biochem J, 2005. **386**(Pt 2): p. 201-14.
9. Molli, P.R., et al., *PAK signaling in oncogenesis.* Oncogene, 2009. **28**(28): p. 2545-55.
10. Lei, M., et al., *Structure of PAK1 in an autoinhibited conformation reveals a multistage activation switch.* Cell, 2000. **102**(3): p. 387-97.
11. Chong, C., et al., *The mechanism of PAK activation. Autophosphorylation events in both regulatory and kinase domains control activity.* J Biol Chem, 2001. **276**(20): p. 17347-53.
12. Kumar, R., A.E. Gururaj, and C.J. Barnes, *p21-activated kinases in cancer.* Nat Rev Cancer, 2006. **6**(6): p. 459-71.
13. Whale, A., et al., *Signalling to cancer cell invasion through PAK family kinases.* Front Biosci (Landmark Ed), 2011. **16**: p. 849-64.
14. Balasenthil, S., et al., *p21-activated kinase-1 signaling mediates cyclin D1 expression in mammary epithelial and cancer cells.* J Biol Chem, 2004. **279**(2): p. 1422-8.
15. Vadlamudi, R.K., et al., *Regulatable expression of p21-activated kinase-1 promotes anchorage-independent growth and abnormal organization of mitotic spindles in human epithelial breast cancer cells.* J Biol Chem, 2000. **275**(46): p. 36238-44.
16. Chen, S., et al., *Copy number alterations in pancreatic cancer identify recurrent PAK4 amplification.* Cancer Biol Ther, 2008. **7**(11): p. 1793-802.
17. Callow, M.G., et al., *Requirement for PAK4 in the anchorage-independent growth of human cancer cell lines.* J Biol Chem, 2002. **277**(1): p. 550-8.
18. Tang, Y., et al., *A role for Pak protein kinases in Schwann cell transformation.* Proc Natl Acad Sci U S A, 1998. **95**(9): p. 5139-44.
19. Chow, H.Y., et al., *p21-Activated kinase 1 is required for efficient tumor formation and progression in a Ras-mediated skin cancer model.* Cancer Res, 2012. **72**(22): p. 5966-75.
20. Kikuchi, T., et al., *In-depth proteomic analysis of nonsmall cell lung cancer to discover molecular targets and candidate biomarkers.* Mol Cell Proteomics, 2012. **11**(10): p. 916-32.
21. Ong, C.C., et al., *Targeting p21-activated kinase 1 (PAK1) to induce apoptosis of tumor cells.* Proc Natl Acad Sci U S A, 2011. **108**(17): p. 7177-82.
22. Rettig, M., et al., *PAK1 kinase promotes cell motility and invasiveness through CRK-II serine phosphorylation in non-small cell lung cancer cells.* PLoS One, 2012. **7**(7): p. e42012.
23. Zhang, S., et al., *The tumor suppressor LKB1 regulates lung cancer cell polarity by mediating cdc42 recruitment and activity.* Cancer Res, 2008. **68**(3): p. 740-8.
24. Mortazavi, F., et al., *Significance of KRAS/PAK1/Crk pathway in non-small cell lung cancer oncogenesis.* BMC Cancer, 2015. **15**: p. 381.
25. Kris, M.G., et al., *Efficacy of gefitinib, an inhibitor of the epidermal growth factor receptor tyrosine*

kinase, in symptomatic patients with non-small cell lung cancer: a randomized trial. JAMA, 2003. **290**(16): p. 2149-58.
26. Lynch, T.J., et al., *Activating mutations in the epidermal growth factor receptor underlying responsiveness of non-small-cell lung cancer to gefitinib.* N Engl J Med, 2004. **350**(21): p. 2129-39.
27. Paez, J.G., et al., *EGFR mutations in lung cancer: correlation with clinical response to gefitinib therapy.* Science, 2004. **304**(5676): p. 1497-500.
28. Soda, M., et al., *Identification of the transforming EML4-ALK fusion gene in non-small-cell lung cancer.* Nature, 2007. **448**(7153): p. 561-6.
29. Shaw, A.T., et al., *Clinical features and outcome of patients with non-small-cell lung cancer who harbor EML4-ALK.* J Clin Oncol, 2009. **27**(26): p. 4247-53.
30. Kwak, E.L., et al., *Anaplastic lymphoma kinase inhibition in non-small-cell lung cancer.* N Engl J Med, 2010. **363**(18): p. 1693-703.
31. Ballman, K.V., *Biomarker: Predictive or Prognostic?* J Clin Oncol, 2015. **33**(33): p. 3968-71.
32. Ettinger, D.S., et al., *Non-Small Cell Lung Cancer, Version 5.2017, NCCN Clinical Practice Guidelines in Oncology.* J Natl Compr Canc Netw, 2017. **15**(4): p. 504-535.
33. Riely, G.L., *What, When, and How of Biomarker Testing in Non-Small Cell Lung Cancer.* J Natl Compr Canc Netw, 2017. **15**(5S): p. 686-688.
34. Scaltriti, M. and J. Baselga, *The epidermal growth factor receptor pathway: a model for targeted therapy.* Clin Cancer Res, 2006. **12**(18): p. 5268-72.
35. Olayioye, M.A., et al., *The ErbB signaling network: receptor heterodimerization in development and cancer.* EMBO J, 2000. **19**(13): p. 3159-67.
36. Stella, G.M., et al., *Targeting EGFR in non-small-cell lung cancer: lessons, experiences, strategies.* Respir Med, 2012. **106**(2): p. 173-83.
37. Araujo, L.H., et al., *Somatic Mutation Spectrum of Non-Small-Cell Lung Cancer in African Americans: A Pooled Analysis.* J Thorac Oncol, 2015. **10**(10): p. 1430-6.
38. Fukuoka, M., et al., *Multi-institutional randomized phase II trial of gefitinib for previously treated patients with advanced non-small-cell lung cancer (The IDEAL 1 Trial) [corrected]*. J Clin Oncol, 2003. **21**(12): p. 2237-46.
39. Perez-Soler, R., et al., *Determinants of tumor response and survival with erlotinib in patients with non--small-cell lung cancer.* J Clin Oncol, 2004. **22**(16): p. 3238-47.
40. Shepherd, F.A., et al., *Erlotinib in previously treated non-small-cell lung cancer.* N Engl J Med, 2005. **353**(2): p. 123-32.
41. Pao, W., et al., *EGF receptor gene mutations are common in lung cancers from "never smokers" and are associated with sensitivity of tumors to gefitinib and erlotinib.* Proc Natl Acad Sci U S A, 2004. **101**(36): p. 13306-11.
42. Sequist, L.V., et al., *Molecular predictors of response to epidermal growth factor receptor antagonists in non-small-cell lung cancer.* J Clin Oncol, 2007. **25**(5): p. 587-95.
43. Pao, W., et al., *Acquired resistance of lung adenocarcinomas to gefitinib or erlotinib is associated with a second mutation in the EGFR kinase domain.* PLoS Med, 2005. **2**(3): p. e73.
44. Kobayashi, S., et al., *EGFR mutation and resistance of non-small-cell lung cancer to gefitinib.* N Engl J Med, 2005. **352**(8): p. 786-92.
45. Hirsch, F.R., et al., *Lung cancer: current therapies and new targeted treatments.* Lancet, 2017. **389**(10066): p. 299-311.
46. Mok, T.S., et al., *Osimertinib or Platinum-Pemetrexed in EGFR T790M-Positive Lung Cancer.* N Engl J Med, 2017. **376**(7): p. 629-640.
47. Attarian, S., N. Rahman, and B. Halmos, *Emerging uses of biomarkers in lung cancer management: molecular mechanisms of resistance.* Ann Transl Med, 2017. **5**(18): p. 377.
48. Katayama, R., C.M. Lovly, and A.T. Shaw, *Therapeutic targeting of anaplastic lymphoma kinase in lung cancer: a paradigm for precision cancer medicine.* Clin Cancer Res, 2015. **21**(10): p. 2227-35.

49. Soda, M., et al., *A mouse model for EML4-ALK-positive lung cancer.* Proc Natl Acad Sci U S A, 2008. **105**(50): p. 19893-7.
50. Peters, S., et al., *Alectinib versus Crizotinib in Untreated ALK-Positive Non-Small-Cell Lung Cancer.* N Engl J Med, 2017. **377**(9): p. 829-838.
51. Rikova, K., et al., *Global survey of phosphotyrosine signaling identifies oncogenic kinases in lung cancer.* Cell, 2007. **131**(6): p. 1190-203.
52. Lin, J.J. and A.T. Shaw, *Recent Advances in Targeting ROS1 in Lung Cancer.* J Thorac Oncol, 2017. **12**(11): p. 1611-1625.
53. Lin, J.J., et al., *ROS1 Fusions Rarely Overlap with Other Oncogenic Drivers in Non-Small Cell Lung Cancer.* J Thorac Oncol, 2017. **12**(5): p. 872-877.
54. McDermott, U., et al., *Genomic alterations of anaplastic lymphoma kinase may sensitize tumors to anaplastic lymphoma kinase inhibitors.* Cancer Res, 2008. **68**(9): p. 3389-95.
55. Shaw, A.T., et al., *Crizotinib in ROS1-rearranged non-small-cell lung cancer.* N Engl J Med, 2014. **371**(21): p. 1963-71.
56. Pardoll, D.M., *The blockade of immune checkpoints in cancer immunotherapy.* Nat Rev Cancer, 2012. **12**(4): p. 252-64.
57. Freeman, G.J., et al., *Engagement of the PD-1 immunoinhibitory receptor by a novel B7 family member leads to negative regulation of lymphocyte activation.* J Exp Med, 2000. **192**(7): p. 1027-34.
58. Gettinger, S.N., et al., *Overall Survival and Long-Term Safety of Nivolumab (Anti-Programmed Death 1 Antibody, BMS-936558, ONO-4538) in Patients With Previously Treated Advanced Non-Small-Cell Lung Cancer.* J Clin Oncol, 2015. **33**(18): p. 2004-12.
59. Postow, M.A., M.K. Callahan, and J.D. Wolchok, *Immune Checkpoint Blockade in Cancer Therapy.* J Clin Oncol, 2015. **33**(17): p. 1974-82.
60. Sharma, P., et al., *Primary, Adaptive, and Acquired Resistance to Cancer Immunotherapy.* Cell, 2017. **168**(4): p. 707-723.
61. Carbone, D.P., et al., *First-Line Nivolumab in Stage IV or Recurrent Non-Small-Cell Lung Cancer.* N Engl J Med, 2017. **376**(25): p. 2415-2426.
62. Rizvi, H., et al., *Molecular Determinants of Response to Anti-Programmed Cell Death (PD)-1 and Anti-Programmed Death-Ligand 1 (PD-L1) Blockade in Patients With Non-Small-Cell Lung Cancer Profiled With Targeted Next-Generation Sequencing.* J Clin Oncol, 2018. **36**(7): p. 633-641.
63. Paik, P.K., et al., *Clinical characteristics of patients with lung adenocarcinomas harboring BRAF mutations.* J Clin Oncol, 2011. **29**(15): p. 2046-51.
64. Planchard, D., et al., *Dabrafenib plus trametinib in patients with previously untreated BRAF(V600E)-mutant metastatic non-small-cell lung cancer: an open-label, phase 2 trial.* Lancet Oncol, 2017. **18**(10): p. 1307-1316.
65. Odogwu, L., et al., *FDA Approval Summary: Dabrafenib and Trametinib for the Treatment of Metastatic Non-Small Cell Lung Cancers Harboring BRAF V600E Mutations.* Oncologist, 2018.
66. Manser, E., et al., *A brain serine/threonine protein kinase activated by Cdc42 and Rac1.* Nature, 1994. **367**(6458): p. 40-6.
67. Huang, Z., J. Ling, and J.A. Traugh, *Localization of p21-activated protein kinase gamma-PAK/Pak2 in the endoplasmic reticulum is required for induction of cytostasis.* J Biol Chem, 2003. **278**(15): p. 13101-9.
68. Marlin, J.W., et al., *Functional PAK-2 knockout and replacement with a caspase cleavage-deficient mutant in mice reveals differential requirements of full-length PAK-2 and caspase-activated PAK-2p34.* Mamm Genome, 2011. **22**(5-6): p. 306-17.
69. Coniglio, S.J., S. Zavarella, and M.H. Symons, *Pak1 and Pak2 mediate tumor cell invasion through distinct signaling mechanisms.* Mol Cell Biol, 2008. **28**(12): p. 4162-72.
70. Begum, A., et al., *Identification of PAK4 as a putative target gene for amplification within 19q13.12-q13.2 in oral squamous-cell carcinoma.* Cancer Sci, 2009. **100**(10): p. 1908-16.

71. Wen, X., et al., *Knockdown of p21-activated kinase 6 inhibits prostate cancer growth and enhances chemosensitivity to docetaxel.* Urology, 2009. **73**(6): p. 1407-11.
72. Zhang, J.Y., D. Zhang, and E.H. Wang, *Overexpression of small GTPases directly correlates with expression of delta-catenin and their coexpression predicts a poor clinical outcome in nonsmall cell lung cancer.* Mol Carcinog, 2013. **52**(5): p. 338-47.
73. Chang, J.S., et al., *GIT1 promotes lung cancer cell metastasis through modulating Rac1/Cdc42 activity and is associated with poor prognosis.* Oncotarget, 2015.
74. Pitts, T.M., et al., *Association of the epithelial-to-mesenchymal transition phenotype with responsiveness to the p21-activated kinase inhibitor, PF-3758309, in colon cancer models.* Front Pharmacol, 2013. **4**: p. 35.
75. Liu, Y., et al., *The P21-activated kinase expression pattern is different in non-small cell lung cancer and affects lung cancer cell sensitivity to epidermal growth factor receptor tyrosine kinase inhibitors.* Med Oncol, 2016. **33**(3): p. 22.
76. Puto, L.A., et al., *p21-activated kinase 1 (PAK1) interacts with the Grb2 adapter protein to couple to growth factor signaling.* J Biol Chem, 2003. **278**(11): p. 9388-93.
77. Rudolph, J., et al., *Inhibitors of p21-activated kinases (PAKs).* J Med Chem, 2015. **58**(1): p. 111-29.
78. Cancer Genome Atlas Research, N., *Comprehensive molecular profiling of lung adenocarcinoma.* Nature, 2014. **511**(7511): p. 543-50.
79. Gao, J., et al., *Integrative analysis of complex cancer genomics and clinical profiles using the cBioPortal.* Sci Signal, 2013. **6**(269): p. pl1.
80. Cerami, E., et al., *The cBio cancer genomics portal: an open platform for exploring multidimensional cancer genomics data.* Cancer Discov, 2012. **2**(5): p. 401-4.
81. Nelson, M.T., et al., *Preferential, enhanced breast cancer cell migration on biomimetic electrospun nanofiber 'cell highways'.* BMC Cancer, 2014. **14**: p. 825.
82. Johnson, J., et al., *Quantitative analysis of complex glioma cell migration on electrospun polycaprolactone using time-lapse microscopy.* Tissue Eng Part C Methods, 2009. **15**(4): p. 531-40.
83. Murray, B.W., et al., *Small-molecule p21-activated kinase inhibitor PF-3758309 is a potent inhibitor of oncogenic signaling and tumor growth.* Proc Natl Acad Sci U S A, 2010. **107**(20): p. 9446-51.
84. Radu, M., et al., *PAK signalling during the development and progression of cancer.* Nat Rev Cancer, 2014. **14**(1): p. 13-25.
85. Giese, A., et al., *Dichotomy of astrocytoma migration and proliferation.* Int J Cancer, 1996. **67**(2): p. 275-82.
86. Jang, I., et al., *Pak1/LIMK1/Cofilin Pathway Contributes to Tumor Migration and Invasion in Human Non-Small Cell Lung Carcinomas and Cell Lines.* Korean J Physiol Pharmacol, 2012. **16**(3): p. 159-65.